DNB Working Paper

No 827/January 2025

Untangling Illiquidity: Optimal Asset Allocation with Private Asset Classes

Daniel Dimitrov

DeNederlandscheBank

EUROSYSTEEM

Untangling Illiquidity: Optimal Asset Allocation with Private Asset Classes

Daniel Dimitrov *

* Views expressed are those of the author and do not necessarily reflect official positions of De Nederlandsche Bank.

Working Paper No. 827

January 2025

De Nederlandsche Bank NV
P.O. Box 98
1000 AB AMSTERDAM
The Netherlands

Untangling Illiquidity: Optimal Asset Allocation with Private Asset Classes

Daniel Dimitrov[*†]

January 30, 2025

Abstract

This paper examines the asset allocation problem faced by long-term investors seeking exposure to illiquid private assets. Liquidity uncertainty hampers continuous rebalancing and withdrawals, while illiquidity risk premia can lead to unintended overallocation during extended periods of asset lock-ups, increasing the variability of portfolio consumption and shrinking investor welfare. Using a dynamic allocation model calibrated on analyst-based capital market expectations, I find that while adding private assets to the investment universe may offer benefits, ignoring illiquidity in the portfolio construction process leads to substantial welfare losses.

JEL codes: D81,G11,G12,E21

Keywords: asset allocation, (il)liquidity, private assets, model misspecification

---

[*]De Nederlandsche Bank, University of Amsterdam; e-mail: d.k.dimitrov@uva.nl.

[†]I would like to thank Roel Beetsma and Dirk Broeders for extensive comments in earlier drafts of the paper; and Aleksandar Andonov, Matteo Bonetti, Damiaan Chen, Thierry Foucault, Frank de Jong (discussant), Reinier Goudswaard, Felix Kübler, Kostas Mavromatis, Bertrand Melenberg, Albert J. Menkveld, J.M. Schumacher, Christian Stoltenberg, Sweder van Wijnbergen, Bas Werker, and participants in the Market Microstructure Summer School 2021, MAF 2024, QFFE 2024, Netspar 2024 conferences for the valuable feedback and suggestions. The code to reproduce the model presented in this paper is available at https://github.com/danielkdimitrov/portfolioChoiceIlliq. The views expressed here are those of the author and do not reflect the views of De Nederlandsche Bank, or the Eurosystem.

1 Introduction

Institutional investors, such as pension funds, sovereign wealth funds, and endowments, have endorsed private asset classes into their portfolios in search of improved risk-adjusted returns and diversification (Andonov et al., 2015, 2021, 2023; Broeders et al., 2021; Giesecke and Rauh, 2023; Begenau et al., 2024). The conventional wisdom states that these investors' long horizons allow them to capitalize on the illiquidity premia (potentially) offered by private assets.

Yet, non-traditional asset categories, such as private equity, private real estate, infrastructure investments, and hedge funds, pose a challenge to the established asset allocation methods. While the literature to address this is growing (Terhaar et al., 2003; Luxenberg et al., 2022; Korteweg and Westerfield, 2022; Dimmock et al., 2023), there is still a lack of theoretical underpinning and practical understanding of what these challenges entail for the investor and how to embed them in the portfolio construction process.

In this paper, I highlight the risk of illiquidity, the fact that private asset classes typically lock up invested funds for an uncertain period. This restricts investors from fully accessing liquidity within their portfolio and hampers their ability to rebalance towards the strategic allocation targets as asset shares drift over time. I extend the dynamic portfolio choice model of Ang et al. (2014) and adapt it to address the strategic asset allocation (SAA) problem of a long-term investor who wants to allocate to illiquid private assets. Calibrating the model on publicly available capital market assumptions (CMAs), I then solve for the optimal allocation to several private asset classes and quantify the welfare improvements they provide to an investor already holding a diversified liquid portfolio. Additionally, I evaluate the welfare losses associated with constructing a portfolio when liquidity risk is ignored. In doing so, I provide a fast and tractable numerical algorithm to solve the underlying dynamic optimization problem, thus demonstrating the model's practicality.

Liquidity in this model arrives randomly through Poisson shocks, calibrated to the expected period over which the funds in the private asset classes are not redeemable.

The uncertainty surrounding the timing of liquidity events affects the investor's optimal allocation decision in several ways. In anticipation of prolonged periods of illiquidity for the private assets, it is optimal for the investor to preemptively reduce the portfolio consumption (withdrawal) rate and to tilt in advance the strategic asset weights away from the illiquid investment as a way of reducing the exposure to this additional source of risk. In addition, when the private asset has a publicly traded equivalent in the investment universe, a substitution effect is observed, by which the publicly traded substitute is preferred in the SAA instead of the private asset exposure.

I find that the attributes often cited as advantages of private assets — higher returns and diversification potential — are also the factors that interact negatively with illiquidity risk. Low correlation with the rest of the portfolio leads to a reduced possibility of hedging the volatility of the share in private illiquid assets. Consequently, the investor must secure additional risk-free buffers to mitigate the increased variability in portfolio consumption caused by fluctuations in the value of the private asset. This strategy ensures that negative shocks from publicly traded risky assets do not deplete liquidity, and preserves consumption during periods when a large part of the investor's wealth is locked in illiquid allocations. A higher expected return of the private asset, on the other hand, due to the presence of illiquidity premia, leads to unintended overallocation through extended periods of illiquidity, as in expectation the share invested in the illiquid private asset rises above its SAA target.

Overall, I find that private equity, infrastructure investments, private real estate, and diversified hedge funds improve the Certainty Equivalent Consumption (CEC) of an optimizing investor with a CRRA utility who has a moderate risk appetite and already holds a diversified portfolio of stocks, bonds, and public real estate. Despite being economically substantial, these improvements are significantly tempered when illiquidity risk is taken into account. Yet, institutional investors widely use SAA optimization approaches that quantify risk purely from an asset volatility angle (Kim et al., 2021; Begenau et al., 2024). Ignoring the liquidity aspects of private assets thus exposes them to the risk of sub-optimal and overoptimistic allocation to private assets. Mimicking an investor who constructs her portfolio through a mean-variance lens without a view on illiquidity risk, I find a considerable welfare loss associated with the highly illiquid private asset classes: private equity, infrastructure, and real estate, a negligible loss for the relatively more liquid private asset classes, such as hedge funds.

The paper continues as follows: Section 2 reviews the existing literature, Section 3 outlines the model; Section 4 shows the key properties of the solution in a controlled stylized setting; Section 5 applies the model to analyst CMAs and evaluates the welfare benefits and misallocation costs associated with illiquid private assets; Annex A outlines the numerical approaches used to solve the presented dynamic portfolio choice model.

2 Related Literature

This paper contributes to two separate strands of the investment literature. The first one, on the practical side, e.g. Terhaar et al. (2003); Ilmanen et al. (2020), discusses optimal portfolio construction, emphasizing the importance of forward-looking capital market assumptions and cautioning against the pitfalls of smoothed reported returns of illiquid private investments. The current paper goes a step further by explicitly incorporating illiquidity risk into the SAA process, thus parting from the widely used static mean-variance optimization approaches.

On the other hand, I relate to the theoretical finance literature which examines dynamic portfolio choice with liquidity frictions. These are broadly classified along three main dimensions: transaction costs (Zabel, 1973; Magill and Constantinides, 1976; Gennotte and Jung, 1994; Boyle and Lin, 1997; Dai et al., 2011), delayed execution (Longstaff, 2001), and inability to access a market in periods of deterministic (Miklós and Ádám, 2002; Dimmock et al., 2023) or, most closely related to the approach taken here, stochastic (Ang et al., 2014; Jansen and Werker, 2022) time length. The methodological contribution of this paper is to extend the dimensionality of the asset allocation problem and to provide a fast numerical solution approach to the arising dynamic programming problem.

Ang et al. (2014) extend the Merton (1971) continuous-time dynamic portfolio approach by incorporating a Poisson process which governs the random availability of trading opportunities for the illiquid asset. This is motivated by over-the-counter (OTC) markets and the random time it takes to find a trading counterparty. Random waiting time is a feature that often arises in the literature on search frictions, such as in Diamond (1982). Jansen and Werker (2022) then extend the framework further to account for limited investment horizons and solve for the shadow cost of illiquidity, i.e. the return premia which put at par (in utility-equivalent terms) the illiquid private asset and its liquid public equivalent. My approach is different; I quantify the overall benefit of including the illiquid private asset in the investment universe vs. not including it at all; I evaluate the extent to which various illiquid private asset classes can be substituted by a set of publicly traded ones. For this purpose, I extend the dynamic portfolio choice problem with a larger number of assets in the investment universe, bringing the model closer to a practical implementation. The curse of dimensionality makes such problems harder to solve, and large dimensions are typically avoided in previous literature, keeping the dynamic models stylized in nature. Yet, a wider diversity in the investment universe offers more opportunities to substitute the costly (from a risk point of view) illiquid assets, so it becomes important to develop the model to cover multiple assets. For this purpose, I adapt the numerical algorithms provided by Cai et al. (2013) to take into account stochastic liquidity opportunities rather than only fixed transaction costs. The numerical methodology thus relies on multi-variate quadrature approximations and value function iteration to solve a non-trivial portfolio choice problem.

This paper also adds to the recent and growing literature on portfolio allocation with private equity (PE) funds, as reviewed in Korteweg and Westerfield (2022). This body of work typically breaks down the distinctive cash flow structure of private equity, consisting of capital calls, dividend payouts, and fees, into components that can be modeled. For example, Gourier et al. (2024) and Giommetti and Sorensen (2021) both develop dynamic portfolio allocation models to examine the welfare implications of ex-ante capital commitments to the PE fund, with the former study using Poisson processes to model capital calls and dividend payouts, and the latter assuming that calls happen gradually.

Dimmock et al. (2023) suggest that the illiquidity of PE investments can be diversified through a dynamic strategy with staggered asset lock-up expirations, though this poses constraints for most investors, who typically hold only one or two PE managers (Gredil et al., 2020). Luxenberg et al. (2022) deviate from the dynamic programming formulation of the allocation problem and propose a model predictive control approach for solving it. My approach simplifies the liquidity features of private assets by assuming that during liquidity events, the portfolio can be rebalanced freely to target allocations. For PE, intermediate cash flows may provide partial liquidity along the life of the investment, but these generally occur later in the lifecycle of the fund, making the assumption of a single liquidity event a reasonable approximation. However, through this simplification, the model is fully capable of being calibrated on CMAs consisting of expected returns and a covariance matrix, with only one additional dimension needed — the expected timing of the liquidity event. This makes the model easy to implement by institutional investors who already use a mean-variance approach to the SAA process.

3 Model

The representative long-term investor in this model is infinitely lived and has a CRRA utility over the consumption amount C_t:

$$u(C_t) = \frac{C_t^{1-\gamma}}{1-\gamma} \tag{1}$$

with time $t \geq 0$ as a time index, and $\gamma > 0, \gamma \neq 1$ as the coefficient of relative risk aversion, where higher γ implies a higher risk aversion. The investor constructs a portfolio of risky assets. Consumption is then funded out of this portfolio with no other intermediate income.

The investment universe: The instantaneous risk-free rate is fixed. Denoting it as r, the price B_t of a risk-free asset then follows the process:

$$dB_t/B_t = r dt \tag{2}$$

In addition, there are n marketable risky assets. The vector of their returns $\boldsymbol{dS}/\boldsymbol{S}$ evolves as a multivariate Geometric Brownian Motion process such that:

$$\frac{\boldsymbol{dS}_t}{\boldsymbol{S}_t} = \boldsymbol{\mu} dt + \boldsymbol{\sigma} \boldsymbol{dZ}_t \tag{3}$$

where $\mathbb{1}$ stands for a n-dimensional column vector of ones, $\boldsymbol{dZ}_t$ is a vector of n independent Brownian motions supported by probability space $(\Omega, \Im, \mathbb{P})$; $\boldsymbol{\mu}$ is a $n \times 1$ vector of expected returns; $\boldsymbol{\sigma}$ is $n \times n$ lower triangular matrix holding the sensitivities of the risky asset returns to the Brownian uncertainties with $\boldsymbol{\Sigma} = \boldsymbol{\sigma}\boldsymbol{\sigma}'$ representing the corresponding variance-covariance matrix; $\boldsymbol{\lambda} = \boldsymbol{\sigma}^{-1}(\boldsymbol{\mu} - r\mathbb{1})$ is the price of risk.

Introducing the illiquid private asset: Assume now that the asset corresponding to the n-th row in the vector specification (3) is not marketable all the time. A market opportunity for it arises only when a Poisson process N_t with intensity η hits. The Poisson process is independent of the Brownian motions defined earlier. Also, in the limit, when $1/\eta \to 0$, the private asset approaches full liquidity, and the solution of the model will resemble the Merton portfolio choice problem. On the other hand, as $1/\eta \to \infty$, the private asset is never liquid, and the solution will converge to a Merton portfolio choice problem in which the private asset is completely excluded from the investment universe.

To keep track of liquid and illiquid assets, we define the partitioned vector of expected asset returns and the partitioned matrix of sensitivities to the respective Brownian motions driving asset volatility:

$$\boldsymbol{\mu} = \begin{bmatrix} \boldsymbol{\mu}_w \\ \mu_x \end{bmatrix}, \boldsymbol{\sigma} = \begin{bmatrix} \boldsymbol{\sigma}_w \\ \boldsymbol{\sigma}_x \end{bmatrix} \tag{4}$$

where $\boldsymbol{\mu}_w$ is a $(n-1) \times 1$ vector that captures the expected return of the liquid assets; μ_x is the drift of the illiquid asset; $\boldsymbol{\sigma}_w$ and $\boldsymbol{\sigma}_x$ are respectively $(n-1) \times n$ and $1 \times n$ matrices that capture the sensitivities respectively of the liquid assets and the illiquid asset to the Brownian motions.

Some of the implications of this construction are worth discussing before proceeding with the model. First, by construction, arrivals of the liquidity opportunities embedded in the Poisson structure are i.i.d over time. While this may be problematic over very short horizons in which clustering, autocorrelation or liquidity spillover effects may be present, these are less likely to play a role for long-term investors. A second simplification is to assume that even though the private asset is illiquid, the investor can continuously observe the evolution of its value over time, and when the exogenous Poisson shock hits, the investor is able to realize this value. While in reality information frictions may be present on a manager level (Sefiloglu, 2022), they are outside the scope of the asset allocation problem, which ignores manager level frictions and focuses on aggregate asset classes, assuming that the risk and return parameters of the model once calibrated to the CMAs will already account for any such losses.

In the context of private asset classes, the random nature of liquidity arrivals (or correspondingly, the periods of random length of illiquidity) can be interpreted in several ways. Private equity, real estate, and infrastructure funds have uncertain dividend payouts and it takes years to fully redeem investments (Metrick and Yasuda, 2010). Hedge funds often have "gates" through which managers can at discretion restrict investor liquidity to prevent a run on the fund (Darolles and Roussellet, 2023). Additionally, hedge funds impose varying lock-up and notice redemption periods (Schaub and Schmid, 2013). Also, the specific manager who will be delegated to implement a particular SAA exposure is rarely known in advance,[1]. For these reasons, it is reasonable to assume that hedge fund investments also face liquidity that is random within a certain expected waiting

[1]Modern institutions typically follow a structured investment process: first, the investment opportunity set is defined; then, the optimal SAA decision is made based on forward-looking risk-return expectations for the asset classes, along with the investor's constraints and risk tolerance. Only after these parameters are set does the selection of managers for each asset bucket become relevant (see, e.g., Brennan et al. (1997); Martellini and Milhau (2020)).

period at the time strategic allocations are determined.

In all cases, the secondary markets for private asset classes are unreliable and typically involve significant discounts, making them a suboptimal strategy for unlocking liquidity (Gourier et al., 2024). Therefore, I adopt a prudent investment approach which assumes that in constructing the SAAs the investor does not rely on selling the private asset on the secondary market for liquidity.

Investor portfolio dynamics: The investor's total portfolio wealth Q_t can be split into liquid wealth W_t, invested into risky and riskless assets, and illiquid wealth X_t, invested in the illiquid private asset. The only income the investor receives is from the capital gains on the invested wealth. In line with the literature and empirics, the illiquid asset cannot be used as collateral, and as a result, illiquidity cannot be circumvented by pledging the asset and issuing debt instead. The investor controls the asset allocation first through the liquid portfolio composition, defined by the allocation vector $\boldsymbol{\theta}_t$ into liquid risky assets (fractions defined as proportions from liquid wealth); and second, through the transfers dI_t between liquid and illiquid wealth, which are possible only when the Poisson shock hits. The investor can consume directly only out of liquid wealth, so we define the consumption rate as a fraction of liquid wealth: $c_t = \frac{C_t}{W_t}$.

We can write the wealth dynamics of liquid and illiquid wealth as follows:

$$\begin{aligned} dW_t/W_t &= (r + \boldsymbol{\theta}_t'(\boldsymbol{\mu}_w - r\mathbb{1}) - c_t)dt + \boldsymbol{\theta}_t'\boldsymbol{\sigma}_w \boldsymbol{dZ}_t - dI_t/W_t \\ dX_t/X_t &= \mu_x dt + \boldsymbol{\sigma}_x \boldsymbol{dZ}_t + dI_t/X_t \end{aligned} \tag{5}$$

Naturally, then we have $dQ_t = dW_t + dX_t$.

Value function: The value function for a utility-maximizing dynamic investor, subject to the wealth dynamics above, can then be written as

$$V(W_t, X_t) = \sup_{\theta_s, dI_s, c_s} E_t \int_t^{\infty} \mathrm{e}^{-\beta(s-t)} u(C_s) ds \tag{6}$$

which (as shown in Annex C.2) yields the HJB equation:

$$\mathcal{L}^C + \mathcal{L}^\theta + \mathcal{L} - \beta V(W_t, X_t) = 0$$

where

$$\mathcal{L}^C = \sup_{C_t} \left\{ u(C_t) - C_t V_W \right\} \tag{7}$$

$$\mathcal{L}^\theta = \sup_{\theta_t} \left\{ (r + \boldsymbol{\theta}_t'(\boldsymbol{\mu}_w - r\mathbb{1}) V_W W_t + \frac{1}{2} V_{WW} W_t^2 \boldsymbol{\theta}_t' \boldsymbol{\sigma}_w \boldsymbol{\sigma}_w' \boldsymbol{\theta}_t + V_{WX} W_t X_t \boldsymbol{\theta}_t' \boldsymbol{\sigma}_w \boldsymbol{\sigma}_x' \right\} \tag{8}$$

$$\mathcal{L} = V_X \mu_x + \frac{1}{2} V_{XX} X^2 \boldsymbol{\sigma}_x \boldsymbol{\sigma}_x' + \eta \left(V^* - V(W_t, X_t) \right) \tag{9}$$

Denote the share of illiquid wealth (the allocation to the private illiquid asset) as:

$$\xi_t = \frac{X_t}{Q_t} \tag{10}$$

Using the homogeneity property of the value function, following from the homogeneity of the CRRA utility (see Annex C.1), we can factor out total wealth and define a reduced value function as:

$$H(\xi) \equiv V((1-\xi), \xi) = \left(\frac{1}{Q_t} \right)^{1-\gamma} V(W_t, X_t) \tag{11}$$

where $H(\xi_t)$ is a finite, continuous and concave function, maximized at ξ^* for $\xi \in [0, 1)$.[2]

Liquidity opportunity arrives: Whenever liquidity is available, the investor optimizes over the share of illiquid assets, thus moving to the top of the reduced value function $H(\xi_t)$. Then we have the strategic allocation to the illiquid private asset defined as:

$$\xi^* = arg \max_{\xi} H(\xi)$$

This is equivalent to choosing an optimal transfer amount $dI_\tau = (\xi^* - \xi_{\tau^-}) W_{\tau^-}$ where ξ_{τ^-} is the initial illiquid wealth fraction just before rebalancing occurs.

[2]See Ang et al. (2014) for proofs on the properties of this function.

We have transformed the optimization problem (6) from one of finding the value function $V(W_t, X_t)$ itself, into a problem of solving simultaneously for the reduced value function $H(\xi_t)$ and for its maximizing point ξ^*. Furthermore, factoring out total wealth in front of the optimization problems embedded in the HJB equation (7) and (8) shows that the optimal consumption and allocation to liquid risky assets can be written as functions of ξ_t and $H(\xi_t)$ (see Annex C.2).

Dynamics during the periods of illiquidity: When the asset remains illiquid, the investor cannot withdraw from or contribute to illiquid wealth, preventing the portfolio from rebalancing to the strategic allocation target of ξ^*. Consequently, between Poisson events, the share of the illiquid private asset fluctuates stochastically with the realized dynamics of the value of the portfolio assets. Also, continuous consumption will drain liquid wealth and increase the share of illiquid assets.

By design, consumption in the periods between the Poisson liquidity arrivals can be funded from liquid wealth only, so by maximizing $\mathcal{L}^C$ we arrive at a modified version of the Envelope Theorem.[3] We can then derive the optimal consumption rate c_t as

$$c(\xi_t) = \Big((1-\gamma)H(\xi_t) - H'(\xi_t)\xi_t\Big)^{-\frac{1}{\gamma}}(1-\xi_t)^{-1} \tag{12}$$

In contrast to the fixed Merton optimal consumption rate in (27), the consumption rate between trading events now is state dependent and varies with ξ_t.

The optimal investment in the risky liquid asset can be derived from (8) also as a reaction function to the illiquid wealth share in the portfolio:

[3]To see that, note that from (7), at optimum, the marginal utility of liquid wealth is equal to the value of a marginal change in liquid wealth, such that

$$u'(C_t) = V_W(W_t, X_t) \iff C_t = I_{u'}\left(V_W(W_t, X_t)\right) = \left(V_W(W_t, X_t)\ \right)^{-\frac{1}{\gamma}}$$

In the CRRA case in particular, $V_W(W_t, X_t) = W_t^{-\gamma}\left((1-\gamma)H(\xi_t) - \xi_t H'(\xi_t)\right)$ and $u'(c_t W_t) = u'((1-\xi_t)W_t) = (1-\gamma)(cW)^{-\gamma}$. To compare this with the benchmark Merton case, see Equation (31) in Annex B.1.

$$\boldsymbol{\theta}(\xi_t) = \underbrace{(\boldsymbol{\sigma}_w \boldsymbol{\sigma}_w')^{-1} (\boldsymbol{\mu}_w - r\mathbb{1}) \underbrace{\left(-\frac{V_W}{V_{WW} W_t}\right)}_{\Phi(\xi_t)}}_{\text{Investment Demand}} + \underbrace{(\boldsymbol{\sigma}_w \boldsymbol{\sigma}_w')^{-1} \boldsymbol{\sigma}_w \boldsymbol{\sigma}_x' \underbrace{\left(-\frac{V_{WX} X_t}{V_{WW} W_t}\right)}_{\Psi(\xi_t)}}_{\text{Hedging Demand}} \tag{13}$$

As a result, the allocation to liquid risky assets can be split into two parts. First is the *investment demand* term, proportional to the liquid assets price of risk, and to an investment curvature term $\Phi(\xi_t)$. The second term we can define as *hedging demand.* Since $\Psi(\xi_t) \leq 0$, this terms is dampening the liquid asset investment demand when the correlation between the liquid sub-portfolio and the illiquid asset is positive, and increases it if the correlation is negative, allowing the investor to hedge some of the volatility of the illiquid private asset through increased liquid asset exposures.[4] [5]

In this set-up, the illiquid allocation with a liquidity event ξ^* and its corresponding allocation of the liquid risky assets $\boldsymbol{\theta}(\xi^*)$ represent the base strategic allocations to which the investor returns whenever the Poisson shock allows. This will define the SAA allocation. In periods of illiquidity, when the allocation to the illiquid asset cannot be adjusted, $\theta(\xi_t)$ will represent the optimal tactical allocation to liquid risky assets as a reaction to the uncontrolled movements in the share of the private asset. The exact functional form of the tactical allocation function will be determined numerically.

Certainty equivalent consumption: Apart from determining the optimal investment and consumption strategies, one additional goal is to compare different investment strategies in utility-equivalent terms. For this purpose, define the lifetime utility value

[4]See Annex C.2 for analytical details into these terms.

[5]To gain intuition into the hedging and the investment terms of the allocation problem, I now simplify the problem and look at a three-asset case with a liquid risk-free asset, liquid public equity, and an illiquid private asset. This brings us back to the original set-up of Ang et al. (2014). Then we have the setup:

$$\boldsymbol{\mu} = \left[\mu_1, \mu_2\right]^\intercal, \boldsymbol{\sigma} = \begin{bmatrix} \sigma_1 & 0 \\ \rho\sigma_2 & \sqrt{1-\rho^2}\sigma_2 \end{bmatrix}, \boldsymbol{\Sigma} = \begin{bmatrix} \sigma_1^2 & \rho\sigma_1\sigma_2 \\ \rho\sigma_1\sigma_2 & \sigma_2^2 \end{bmatrix}$$

The *investment demand* in the liquid risky asset then is given by $\frac{\mu_1 - r}{\sigma_1^2}\Phi(\xi_t)$. The *hedging demand* term is represented by $\frac{\sigma_2\rho}{\sigma_1}\Psi(\xi_t)$.

generated by guaranteed continuous consumption stream CEC_t fixed at time t as:

$$\int_t^{\infty} \mathrm{e}^{-\beta s} u(CEC_t) ds = \frac{1}{\beta} u(CEC_t)$$

The certainty equivalent consumption (CEC) then is what makes the investor indifferent between the risk-free stream CEC_t and the risky consumption stream underlying a particular investment strategy, so we get:

$$CEC_t \equiv I_u \left(\beta E_t \int_t^{\infty} \mathrm{e}^{-\beta s} u(C_s) ds \right) \tag{14}$$

where $I_u(.)$ stands for the inverse of the utility function. The we can then use the value function from each dynamic investment strategy to value the CEC associated with it. For example, we find that, for the Merton case with consumption rate c_M (see Annex B.1), the CEC per unit of total wealth is:

$$CEC_M = \beta^{\frac{1}{1-\gamma}} \left(\frac{1}{c_M} \right)^{\frac{1}{1-\gamma}}$$

For the illiquid case, the CEC (per unit of total wealth) will depend on the current share of illiquid wealth:

$$CEC_t(\xi) = (\beta(1-\gamma) H(\xi_t))^{\frac{1}{1-\gamma}} \tag{15}$$

4 Comparative statics of the private asset allocation

This section examines the model solution properties under a controlled setting which disentangles the effects coming solely from illiquidity risk by varying the intensity of the Poisson process governing the illiquidity risk and keeping all other properties of the risky assets the same. I consider an investment universe containing a risk-free asset and three risky assets with the same variance and expected return profile. One of the risky assets is not publicly traded and thus is subject to illiquidity risk. In line with the model of illiquidity from Section 3, its allocation can, on average, be adjusted once every $1/\eta$ years. The two liquid risky assets capture the comparative statics of different correlations between the liquid and the illiquid assets and examine the strength of the substitution effect when the illiquidity parameter intensifies.

There are two key assumptions in the baseline case: the private asset does not carry an illiquidity premium, and it is assumed to be uncorrelated to the liquid public assets. Table 1 provides a summary of all the model inputs. The choice for expected return and standard deviation is consistent with the profile of Large Cap US Equity, and the risk-free rate is aligned with the expected return on Money Market funds in the JP Morgan long-term CMAs for 2025 (discussed in detail in Section (5)). The private asset, unless specified otherwise, trades with an intensity of $\eta = 1/10$, implying a rebalancing timeframe of approximately once every ten years. The coefficient of relative risk aversion is set to $\gamma = 6$. This parameterization results in moderately aggressive portfolios - for instance, in the Merton model, the optimizing investor allocates approximately 70% to risky assets (equally distributed between the risky assets) and 30% to the risk-free asset.

There is a debate regarding the size of the liquidity premium and the correlations between private and traditional asset classes. The difficulty in having a straightforward estimates of these parameters lies in the tendency to observe oversmoothed and potentially overstated private asset performance. Metrics like IRR complicate comparisons with public equity equivalents and can be manipulated by private fund managers. Additionally, performance assessment is hampered by infrequent valuations, selection bias (as funds typically trade when successful), and reporting bias (with better-performing funds more likely to disclose their results).[6] For these reasons, I relax the two baseline assumptions and evaluate the comparative statics of the model when the illiquid asset bears a liquidity premium of 3% in line with estimates by Franzoni et al. (2012); and when it has 80% with one of the liquid assets (labeled Public 2), inspired by Franzoni et al. (2012); Ang and Sorensen (2012) who find that private and public equity are highly correlated and exposed to the same underlying risk factors.

[6]See Ang (2014) for further discussion.

Table 1: Baseline parametrization

Parameter	Definition	Default Value
r	risk-free rate	3.1%
β	personal discount rate	3.1%
$\mu_1 = \mu_2 = \mu_3$	risky assets expected return	6.7%
$\sigma_1 = \sigma_2 = \sigma_3$	risky assets volatility	16.2%
ρ	correlation between public asset 2 and the private asset	0 or 0.80
lp	illiquidity premium of the private asset on top of μ_3	0% or 3%
$1/\eta$	average time (in years) between a trading opportunity arises	10
γ	risk aversion parameter in the CRRA utility function	6

Note. The table shows the baseline parameter values used for the comparative statics exercise.

The Value Function: The blue surface in Figure 1a shows the shape of the investor's reduced value function $H(\xi)$ and illustrates its sensitivity to the severity of the private asset illiquidity.[7] A higher $1/\eta$ implies longer expected waiting times before the investor can adjust the allocation of the private asset back to its SAA.

As the expected waiting time increases, the maximum of the value function shifts toward lower allocations to the illiquid private asset ξ, as indicated by the red curve on the surface. This reflects the investor's desire to reduce the strategic allocation to the private asset. For example, when the expected waiting time is 1 year, the optimal allocation to the private asset is 21%. This allocation, however, declines to 5.9% when the waiting time extends to 15 years, reflecting the investor's desire to mitigate illiquidity risk already in the portfolio construction phase.

With higher illiquidity, the value function exhibits greater curvature over the realized allocation of the private asset. As indicated in Equations (12) and (13) this curvature plays a role in the liquid asset allocation and in the consumption rate adjustments during the periods in which liquidity is not available. With longer waiting times, as the realized private asset allocation drifts away from the strategic target, the tactical adjustments become more prominent, and the consumption rate and the risky allocations are reduced

[7] The value function is derived numerically. See the value function iteration and quadrature algorithms described in Annex A.

even with mild deviations of ξ above the strategic target. This effect is illustrated in Figures 1c and 1b.

The shape of the value function also indicates how sensitive investor welfare is with respect to the portfolio share locked up in the private asset. The concavity of the value function implies that under-investing in the private asset would lead to a loss of investor welfare, as a potential source of diversification or return has been underappreciated. At the same time, overallocating would also lead to a loss, as the investor bears more illiquidity risk than is optimal according to their risk preferences. The steeper slope of the value function shows that overallocating to the private asset is having an increasingly negative impact on investor welfare when with higher illiquidity.

Strategic Asset Allocation: Table 2 shows further how the overall strategic portfolio allocations are affected by the severity of the liquidity friction, considering the four cases for the parametrization of the private asset: with and without a liquidity premium, with and without correlation to a public asset from the investment universe. Each table first shows the Merton solution with the full investment universe (row '3m'), hypothesizing that the private asset can always be traded, and the Merton solution only with the two publicly traded assets and cash (row '2m'), hypothesizing that the private asset is excluded from the investment universe. The '2m' case thus serves as a basis for evaluating the improvement in CEC terms of including a private asset in the portfolio. The '3m' provides a ceiling on maximum achievable CEC if the the private asset were fully liquid. The model with illiquidity converges to the '3m' case when the Poisson intensity η is large and converge to the '2m' case when it is small, implying large waiting times between opportunities to rebalance the private asset allocation.

Table 2a looks at a case when the private asset has high diversification potential, i.e. zero correlation to the two public assets. When trading can occur up to a year on average, the optimal allocation with illiquidity is still close to the continuous trading optimal allocation (row '3m') of 22.69%. As the trading friction intensifies, however, the allocation to the private asset is significantly reduced, down to 5.95% with 15 years average waiting

Figure 1: Optimal Solution

(a) Value Function, $-\ln(-H(\xi))$

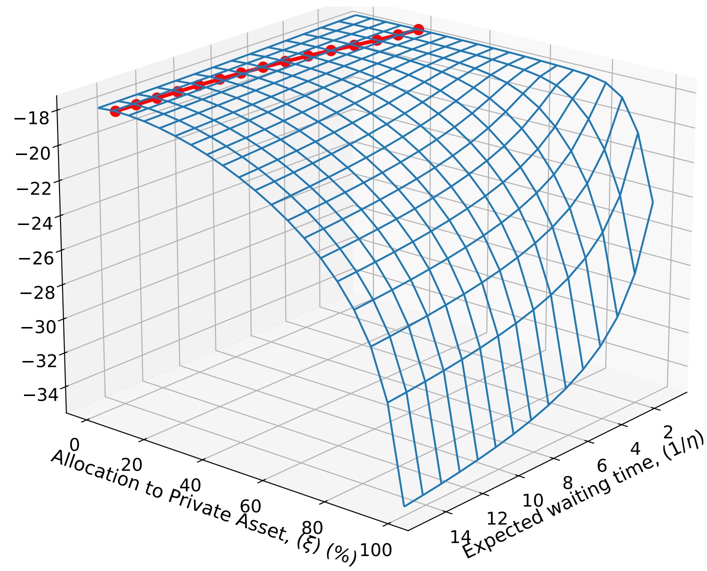

(b) Consumption

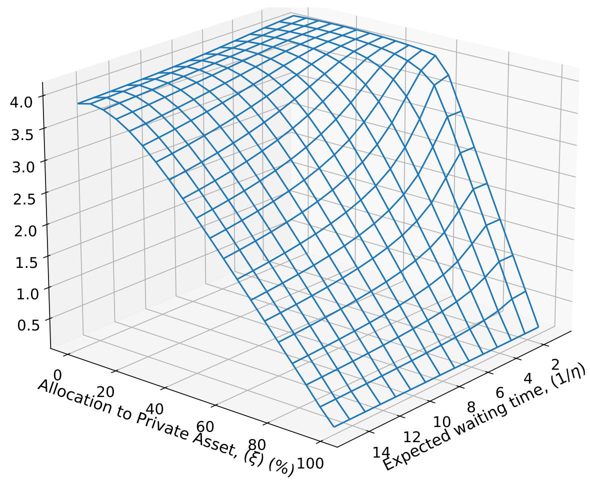

(c) Liquid Risky Alloc.

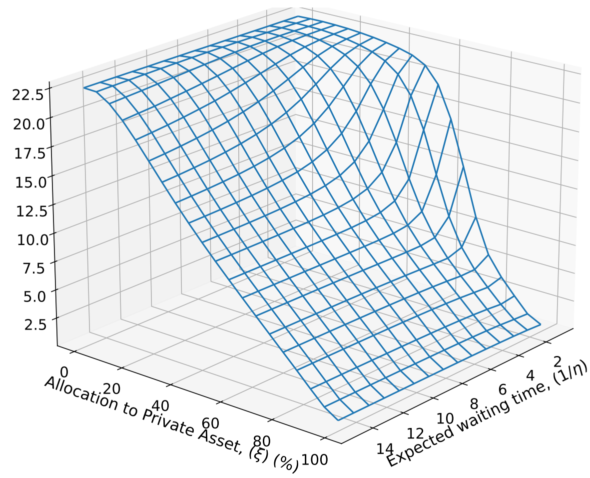

Note. This figure shows the reduced value function sensitivity to the share ξ of the private asset in the portfolio for the different severity of trading friction, $1/\eta$. The red curve on top of the surface highlights the optimizing strategic allocation to the private asset at each level of illiquidity. Panels (b) and (c) show respectively the optimal consumption rate and the the optimal allocation to one of the liquid risky assets (both as % of the total portfolio).

time. Overall, this shift becomes economically significant when the average waiting time is above 2 years. In this baseline case, the reduction in the private asset allocation is not in favor of liquid risky assets, but rather in favor of building stronger cash buffers. This ensures that with prolonged periods of illiquidity the volatility of the public assets will not drain total liquidity from the portfolio, and the investor can still keep robust consumption until the next rebalancing opportunity arrives.

Table 2: Strategic Asset Allocation with a Private Asset

(a) High Diversification ($\rho = 0; lp = 0$)

$1/\eta$	Cash	Public 1	Public 2	Private	CEC
3m	31.92	22.69	22.69	22.69	4.36
0.5	32.77	22.52	22.52	22.19	4.35
1	33.38	22.51	22.51	21.59	4.34
2	34.51	22.49	22.49	20.50	4.33
5	39.60	22.45	22.45	15.50	4.28
10	46.41	22.49	22.49	8.62	4.16
15	49.09	22.49	22.48	5.94	4.09
2m	54.61	22.69	22.69	-	3.93

(b) Low Diversification ($\rho = 0.8; lp = 0$)

$1/\eta$	Cash	Public 1	Public 2	Private	CEC
3m	52.09	22.69	12.61	12.61	3.98
0.5	52.38	22.58	12.72	12.33	3.97
1	52.43	22.58	12.96	12.03	3.97
2	52.56	22.57	13.48	11.39	3.97
5	53.04	22.57	15.52	8.86	3.96
10	53.82	22.57	18.7	4.9	3.95
15	54.22	22.57	20.29	2.92	3.94
2m	54.61	22.69	22.69	-	3.93

(c) High Diversification, Premium ($\rho = 0; lp = 0.03$)

$1/\eta$	Cash	Public 1	Public 2	Private	CEC
3m	13.01	22.69	22.69	41.61	5.40
0.5	14.83	22.38	22.38	40.41	5.37
1	15.95	22.34	22.34	39.37	5.36
2	20.56	22.24	22.24	34.96	5.30
5	35.24	22.20	22.20	20.35	4.91
10	43.70	22.33	22.33	11.64	4.55
15	47.27	22.48	22.48	7.78	4.39
2m	54.61	22.69	22.69	-	3.93

(d) Low Diversification, Premium ($\rho = 0.8; lp = 0.03$)

$1/\eta$	Cash	Public 1	Public 2	Private	CEC
3m	41.58	22.69	(29.42)	65.14	5.23
0.5	42.45	22.41	(28.15)	63.29	5.20
1	42.70	22.36	(26.52)	61.46	5.19
2	43.41	22.29	(22.75)	57.05	5.16
5	49.29	22.24	2.92	25.55	4.67
10	51.47	22.33	11.15	15.06	4.39
15	52.52	22.43	14.55	10.50	4.27
2m	54.61	22.69	22.69	-	3.93

Note. This table shows the optimal SAA weights and Certainty Equivalent Consumption (CEC) as a function of the expected waiting time ($1/\eta$, in years) to trade the illiquid asset. The rows $2m$ and $3m$ stand for the continuous-trading Merton case with two and three risky assets, respectively. All numbers are in percentages from total investor wealth.

When the private asset is correlated to a public asset, Public 2 in Table 2b, a **substitution effect** appears - the liquid risky asset displaces the allocation to the correlated private asset. Public asset 2, which is 80% correlated, serves as an effective substitute when the illiquidity in the public asset intensifies. As the diversification benefits in this case are small, we can see that despite the significant relocation from the private asset into Public 2, the CEC losses are not significant, and CEC consumption stays around 3.9% in all cases. In contrast to the diversifying case, however, now cash buffers were already high even when the private asset was fully liquid. The high buffers protect against the individual asset volatility which cannot be dampened in the portfolio through diversification.

Consider the case when the illiquid asset bears a liquidity premium (Tables 2c and 2d). First, when the private asset allocation can be rebalanced relatively frequently (less than 2 years on average) and a well-correlated publicly traded equivalent exists (Public 2 in Table 2d), the investor sells short the public equivalent and allocates the proceeds to the illiquid private asset. This exploits the opportunity to harvest the illiquidity premia of the private asset while also hedging its volatility through the short position in its public equivalent. However, as the time to trade the illiquid asset extends beyond five years, this strategy becomes suboptimal, and the investor transitions to a long-only portfolio. The optimal allocation still amounts to about 10% in the private asset when illiquidity is extremely low, indicating an ability of the investor to still accommodate the illiquidity risk associated with the private asset. Note that in this case the substitution effect observed earlier now works in reverse - the investor prefers the higher yielding private asset and allocates less to Public 2 compared to the case when the illiquid asset has zero correlation with it.

The Distribution of ξ: The dynamics of ξ over time are driven by several forces. While the investor can return to the optimal SAA levels ξ^* when a liquidity opportunity arises, the rest of the time the realized allocation drifts freely based on the how the value of the liquid subportfolio changes relative to the value of the illiquid allocation. In addition, the continuous consumption out of liquid wealth creates an additional tendency for the illiquid allocation to grow relative to the liquid one. Figure 2a shows a density plot of the realized ξ for a simulated time path of the optimal investment portfolio under the baseline case. In both the five-year and the 15-year liquidity waiting time, most of the distribution mass of the realized allocation is concentrated just above the SAA value ξ^* indicated by the vertical dotted line. As expected, in the 15-year waiting time, the optimal SAA to the private asset decreases. At the same time, the right tail of the realized allocation to the private asset becomes fatter, indicating that while the investor has preemptively reduced the strategic allocation to the private asset compared to the more liquid case, there is still a growing likelihood of extreme unintended over-allocation to the private asset. Figure 2b further shows that the tendency for over-allocation becomes particularly pronounced when the private asset carries a high liquidity premium. Especially in the 15-year case, the median realized allocation to private assets is clearly above the strategic level (the dotted vertical line at ξ^*), reflecting the persistent drift in ξ caused by the prolonged illiquidity periods and the tendency for outperformance of the illiquid asset.

Figure 2: The Density of Realized Private Asset Allocation

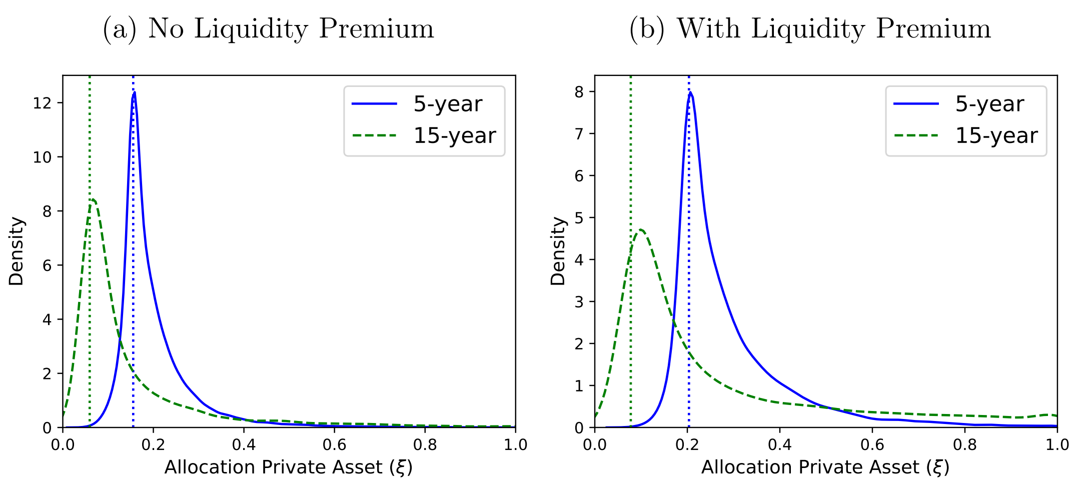

Note. Figures (a) and (b) show kernel plots of the realized allocation to the private asset without and respectively with an illiquidity premium for the private asset. The vertical dotted lines indicate the strategic allocation, ξ^*. The results are based on model simulation.

Optimal consumption and illiquidity-related consumption variability: Table 3 highlights through a simulation how illiquidity risk impacts the realized allocation to the private asset and the realized consumption rate. In each case, the table shows a 95% range and the median of each variable in a model simulation. To put the risk of illiquidity in perspective, the numbers in bold show cases in which the realized consumption falls below the benchmark Merton optimal consumption of 3.78% evaluated when the private assets are excluded from the investment universe. As the waiting time of liquidity increases above two years, reasonable tail scenarios start appearing in which the investor needs to significantly curb consumption due to portfolio liquidity dry-ups.

This risk of over-allocating to the private asset and consequently experiencing a liquidity dry-up becomes particularly notable with prolonged expected waiting times between rebalancing opportunities combined with an illiquidity premium on the private asset (tables 3c and 3d). In those cases, we observe that the 97.5 percentiles of the realized private asset allocation increase substantially. The risk appears that the private asset may dominate the whole portfolio without the investor being able to rebalance back to the strategic targets.

Table 3: Private Asset SAA and Consumption Rate, 95% Range of Realized Scenarios

(a) $\rho = 0; lp = 0$

	Allocation, ξ			Consumption Rate		
$1/\eta$	2.5%	50%	97.5%	2.5%	50%	97.5%
0.5	19.14	22.19	27.13	4.12	4.12	4.12
1	17.75	21.59	30.18	4.11	4.12	4.12
2	15.62	20.74	35.05	4.08	4.11	4.11
5	11.09	17.60	46.18	**3.59**	4.06	4.07
10	5.75	11.21	56.83	**2.42**	3.96	3.97
15	3.64	8.46	61.26	**1.97**	3.90	3.92

(b) $\rho = 0.8; lp = 0$

	Allocation, ξ			Consumption Rate		
$1/\eta$	2.5%	50%	97.5%	2.5%	50%	97.5%
0.5	10.75	12.33	15.11	3.82	3.82	3.82
1	9.98	12.03	16.9	3.82	3.82	3.82
2	8.9	11.61	19.65	3.82	3.82	3.82
5	6.27	9.96	27.37	**3.76**	3.81	3.82
10	3.59	6.45	36.92	**3.29**	3.80	3.80
15	2.08	4.38	42.92	**2.81**	3.79	3.80

(c) $\rho = 0.8; lp = 0.03$

	Allocation, ξ			Consumption Rate		
$1/\eta$	2.5%	50%	97.5%	2.5%	50%	97.5%
0.5	36.85	40.41	48.72	4.91	4.91	4.91
1	34.84	39.37	54.33	4.88	4.90	4.91
2	29.82	36.92	60.99	4.54	4.86	4.86
5	16.33	24.83	70.70	**2.50**	4.54	4.57
10	9.10	18.32	87.57	**0.99**	4.21	4.28
15	6.31	15.09	93.95	**0.52**	4.08	4.16

(d) $\rho = 0.8; lp = 0.03$

	Allocation, ξ			Consumption Rate		
$1/\eta$	2.5%	50%	97.5%	2.5%	50%	97.5%
0.5	58.05	63.29	76.19	4.76	4.78	4.81
1	54.16	61.46	84.10	4.64	4.77	4.83
2	48.62	60.28	93.18	4.26	4.75	5.00
5	22.17	31.91	83.99	**2.23**	4.34	4.37
10	13.17	24.56	94.69	**1.09**	4.07	4.15
15	9.41	19.78	98.64	**0.84**	3.97	4.06

Note. This table shows the realized private asset allocations (q values) and consumption rates as a function of the expected waiting time ($1/\eta$, in years) to trade the illiquid asset. The columns $q = 2.5\%$, $q = 50\%$, and $q = 97.5\%$ indicate the quantiles of the respective variables. The numbers in bold show the cases in which the realized consumption falls below the Merton optimal consumption of 3.78% when the private asset is excluded. All numbers are in percentages from total investor wealth.

Next, I compare the consumption rate with an illiquid private asset (solid blue curve in Figure 3) against the consumption rate without it (lower dotted line, derived from the Merton Model), and the consumption rate assuming, hypothetically, that the private asset is fully liquid (upper dashed line, also derived via the Merton Model). The gap between the two horizontal lines shows the overall potential for consumption improvement from the private asset.[8] However, its illiquidity prevents the full realization of this potential and when its share is high, the investor is forced to curb consumption. This is captured by the downward-sloping curve in the right section of the charts. Since illiquidity introduces consumption dependence on the realized private asset holdings, as the realized allocation to the private asset drifts above the strategic optimum, the investor will need to adjust downward the consumption rate below its potential (the diamond at the top of the curve). The shaded grey areas in the figure then show the 95% range of realized consumption rates in a simulated model run. In this line of thinking, Figures 3c and 3d illustrate that the presence of an illiquidity premium substantially increases the consumption potential. At the same time, it also exacerbates the overallocation problem. The widening grey areas reflect the resulting increased variability in realized consumption rates as a response to the overallocation issue. In those cases, also the median allocation rate (indicated by the black dash on the curve) notably exceeds the SAA level (the diamond at the top of the curve). Overall, a higher (ξ^*), particularly driven by the high illiquidity premia or diversification potential in the private asset, also contributes to greater consumption reductions during periods of illiquidity.

Quantifying the benefits of optimal allocation to private assets: Next, we consider the benefits and costs of investing in an illiquid asset. For this purpose, we quantify investor welfare in risk-adjusted terms as the certainty equivalent consumption (CEC) associated with the optimal investment strategy (see Section 3). The CEC with illiquidity

[8] As can be expected, the potential to improve consumption is higher when the private asset offers stronger diversification potential, as in Figure 3a, or when it embeds an illiquidity premium, as illustrated in Figures 3c and 3d. Conversely, Figure 3b demonstrates that a high correlation between the liquid and illiquid assets significantly limits this potential.

Figure 3: Consumption Rates with Private Asset (10-year illiquidity)

(a) $\rho = 0; lp = 0$ (b) $\rho = 0.8; lp = 0$

(c) $\rho = 0; lp = 0.03$ (d) $\rho = 0.8; lp = 0.03$

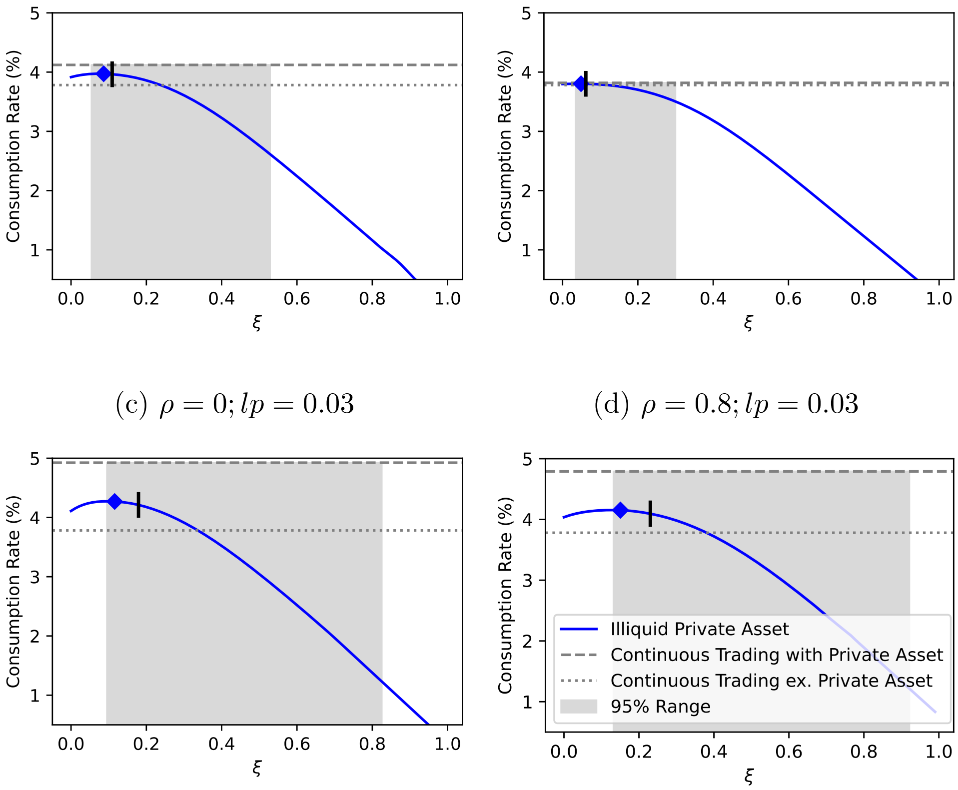

Note. This set of figures illustrates the effects of private asset illiquidity on consumption rates. The solid blue curve represents the consumption rate of an investor holding a private asset with a 10-year average illiquidity; the upper dashed line shows the consumption rates assuming full liquidity of the private asset; and the lower dashed lines show the rate when investment is made in liquid public assets solely. The shaded gray areas denote the 95% range of realized consumption rates, capturing the variability introduced by illiquidity constraints. Panels (a) and (c) assume that the private asset is uncorrelated with any publicly traded asset. Panels (c) and (d) assume a 3% illiquidity premium. The black arrow marks the median realized consumption rate, while the diamond indicates the consumption at the strategic allocation in the private asset.

is a function of the initial allocation ξ_t, as derived in Equation (15). The solid blue curve in Figure 5 illustrates this. Given the dynamic principal of optimality embedded in the model, realizing this CEC is conditional on the investor optimally adjusting the portfolio tactical allocation and returning to the optimal strategic private asset allocation ξ^* given by the model at the next liquidity opportunity. The solid gray line shows this optimal strategic target. The vertical dashed gray line, on the other hand, is the Merton optimal allocation, i.e. assuming that continuous rebalancing opportunities exist for the private asset.

Define the allocation benefit from investing in the private asset class as the improvement in CEC relative to investing only in liquid public assets. Formally:

$$\text{Allocation Benefit} = \frac{CEC(\xi^*)}{CEC_m(\xi = 0)} - 1, \tag{16}$$

where $CEC(\xi^*)$ represents the certainty equivalent consumption with the illiquid asset at its optimal strategic weight, and $CEC_m(\xi = 0)$ corresponds to the CEC when the private asset is excluded from the investment universe altogether, with the optimal policies evaluated through a Merton model.

Figure 4 summarizes the size of this allocation benefits. First, with no liquidity premia (Chart 4a), the allocation benefit is relatively large initially (around 10%) when the private asset is diversifying and highly liquid, but declines gradually when the diversification potential of the asset cannot be fully realized with higher illiquidity. When the asset is not diversifying, the allocation benefit remains minimal, starting at around 1.5% and declining to zero. Factoring in a liquidity premium for the private asset, the benefit declines from 30% to around 10% at the high end of the illiquidity parameter.

Misallocation risk with private assets: Finally, define the misallocation loss as the potential welfare loss from ignoring the illiquidity risk of the private asset. Using the Merton model and assuming erroneously that the private asset allocation is adjustable continuously leads to over-optimistic allocation recommendations, which later on will

Figure 4: Allocation Benefit with Private Asset

(a) No Illiquidity Premium (b) With Illiquidity Premium

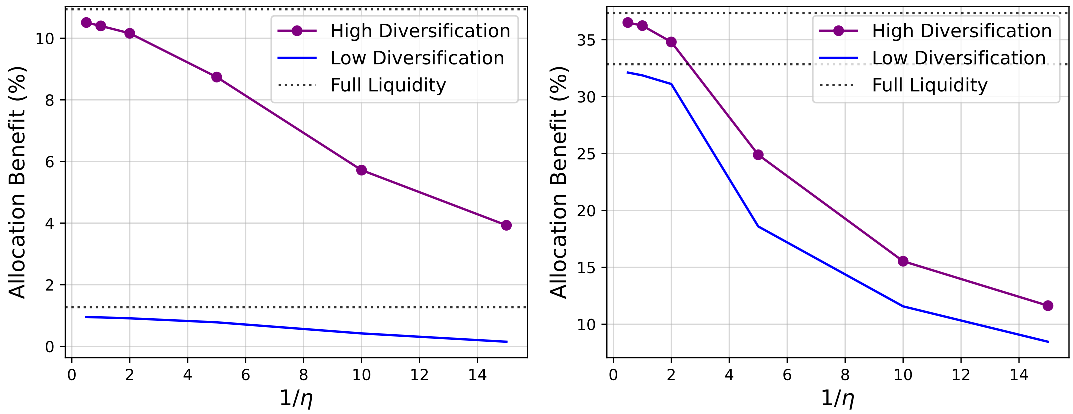

Note. This figure quantifies the benefit of allocating to the illiquid asset. The benefit is measured as the percentage increase in certainty equivalent consumption. Figure (a) shows the benefit when no illiquidity premia exists. Figure (b) specifies 3% illiquidity premia. The dotted lines correspond to the benefit evaluated with a fully liquid asset through the Merton model.

constrain investment consumption. Formally, we define:

$$\text{Misallocation Risk} = -\left(\frac{CEC(\xi^{liquid})}{CEC(\xi^{*})} - 1\right), \tag{17}$$

where $CEC(\xi^{liquid})$ is the CEC in the model with illiquidity at the Merton optimal allocation to private assets, and the $CEC(\xi^{*})$ is evaluated at the optimal allocation with illiquidity properly considered. Note that this formulation of the misallocation risk represents a lower bound on the actual loss. The $CEC(\xi)$ function implicitly assumes that even when the private asset is misallocated the rest of the portfolio and the consumption rate remain optimized.

Judging by the gap between the solid and the dashed vertical lines in Figure 5, the misallocation risk increases with the convexity of the CEC curve and with the properties of the private illiquid asset. When the expected waiting time to rebalance the portfolio is high, or when correlations between the private asset and the liquid assets are lower, the CEC curve becomes more convex. Also, a positive illiquidity premium and low correlation provide over-optimistic Merton allocations, exacerbating the misallocation loss.

Figure 5: Investor Welfare with Private Asset (10-year illiquidity)

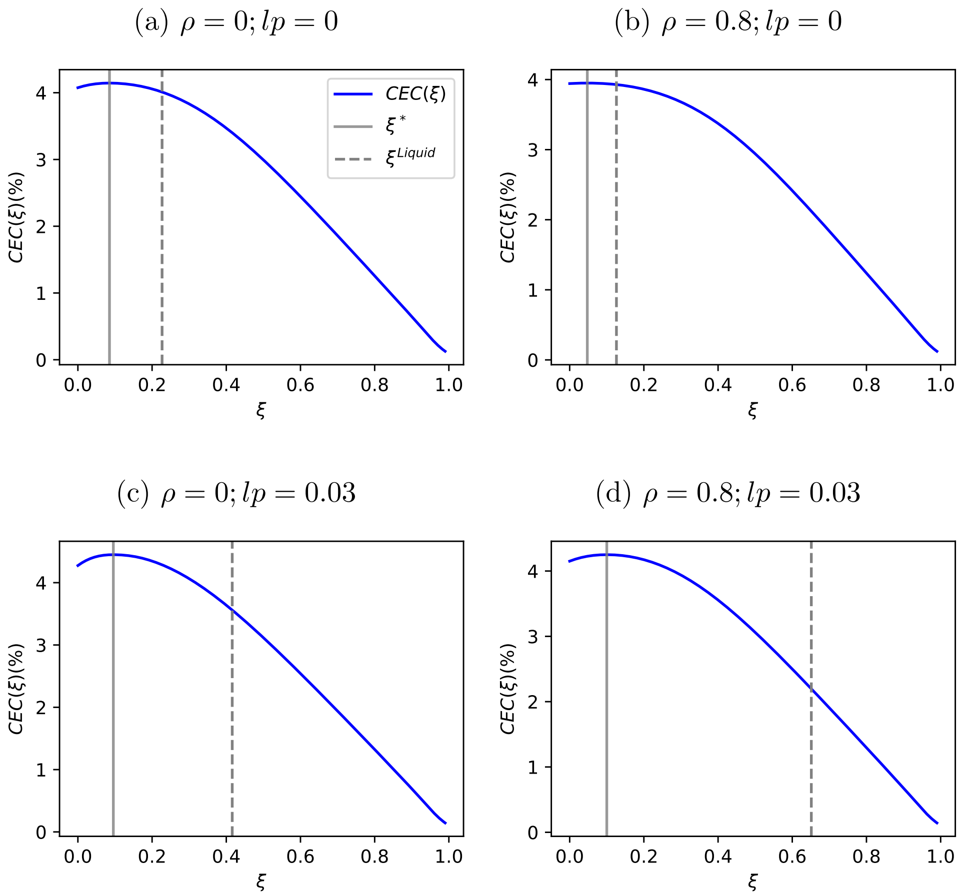

Note. This set of figures illustrates the effects of private asset illiquidity on investor welfare, measured as the Certainty Equivalent Consumption rate as a percent of total wealth. The solid blue curve represents the CEC of an investor holding a private asset with a 10-year average non-trading time as a function of the initial allocation to the private asset, ξ. The dashed vertical lines indicate optimal allocation ignoring liquidity risk. Panels (a) and (c) assume that the private asset is uncorrelated with any publicly traded asset and bears no illiquidity premium. Panels (c) and (d) assume a 3% illiquidity premium. The black arrow marks the median realized consumption rate, while the diamond indicates the consumption at the strategic allocation in the private asset.

5 Strategic Allocation with Private Asset Classes

Next, I part from the stylized calibration of the previous section and evaluate the allocation to private assets based on actual long-term performance expectations. I use the CMAs for 2025 compiled by JP Morgan,[9] who use a combination of quantitative and qualitative inputs and provide a 10-15 year outlook on returns, risks and correlations across various publicly traded and privately asset classes. The private equity projections are net of the fees and expenses charged by managers, so they reflect the final return that can be expected by the investor.[10]

There are two primary reasons to rely on analyst-based capital market assumptions rather than historical asset return data. First, using CMAs in the strategic allocation is a standard practice among institutional investors and is often developed in-house or by consultants by merging insights from quantitative researchers, industry experts, and academics (Andonov and Rauh, 2022; Couts et al., 2023). SAA decisions are inherently forward-looking, making the direct use of historical returns subject parametrization risk to obsolete data (Terhaar et al., 2003). Second, using projections instead of historical data avoids the biases inherent in the historical returns of private asset classes.[11]

In the consequent optimization, the liquid investment universe includes the traditional liquid assets: equity and fixed income. The risk-free asset, represented by the money market rate, is classified under short-term fixed income. I examine five distinct cases, each focusing on a long-only investor. In each separate optimization, I consider adding to the investment universe only one private asset class at a time: Core Real Estate, Infrastructure, Private Equity, or Diversified/Macro Hedge Funds. This approach mirrors

[9] The data is publicly available on JP Morgan's website: https://am.jpmorgan.com/content/dam/jpm-am-aem/global/en/insights/portfolio-insights/ltcma/noindex/ltcma-full-report.pdf

[10] Further details on the approaches used by JP Morgan are available in their methodological guide: https://am.jpmorgan.com/content/dam/jpm-am-aem/global/en/insights/portfolio-insights/ltcma/noindex/ltcma-methodology-handbook.pdf

[11] Infrequent trading tends to over-smooth historical return data, leading to downward-biased estimates of asset variance; secondary markets are often thin, with data frequently derived from appraisals; private equity managers often have discretion over the timing of valuation reporting, creating incentives to disclose performance only when it is favorable; and even when trading occurs, observable market values are more likely to emerge when asset prices are high and sellers are active. For a summary of this evidence, see Ang (2014); Brown et al. (2023, 2019).

an investor interested in exploring a single private asset class out of several alternatives. From a modeling perspective, this also simplifies the analysis by avoiding the complexities of establishing dependencies between multiple Poisson processes across several illiquid asset classes. Table (4) summarizes the input data for the asset classes used in this study.

Table 4: Asset Class Characteristics and Correlation Matrix

Asset Class			**Return**	**Volatility**	**Sharpe**	**Correlation**									
						1	2	3	4	5	6	7	8	9	10
Fixed Income	Money Market*	0	3.1	-	-										
	U.S. Long Treasuries	1	4.3	12.83	0.09										
	U.S. Long Corporate Bonds	2	4.9	12.08	0.15	0.67									
Equity	U.S. Large Cap	3	6.7	16.26	0.22	-0.03	0.47								
	U.S. Small Cap	4	6.9	20.73	0.18	-0.1	0.38	0.9							
	EAFE Equity	5	8.1	17.61	0.28	-0.04	0.52	0.88	0.8						
Liquid Alternatives	U.S. REITs	6	8	17.22	0.28	0.19	0.54	0.77	0.76	0.71					
Private Assets	U.S. Core Real Estate	7	8.1	11.32	0.44	-0.19	-0.02	0.35	0.29	0.27	0.46				
	Global Core Infrastructure	8	6.3	11.01	0.29	0.24	0.2	0.47	0.41	0.55	0.36	0.32			
	Private Equity	9	9.9	19.62	0.35	-0.37	0.26	0.78	0.75	0.8	0.53	0.34	0.62		
	Diversified Hedge Funds	10	4.9	5.80	0.31	-0.21	0.31	0.68	0.64	0.7	0.42	0.32	0.43	0.79	
	Macro Hedge Funds	11	3.8	7.00	0.1	-0.09	0.05	0.16	0.14	0.24	0.1	0.01	0	0.26	0.48

Note. This table shows the Capital Market Assumptions based on the JP Morgan's report for 2025. These include the expected (net) returns, standard deviations of the asset classes considered here, and the correlations between them.

The expected waiting times associated with the illiquid private assets are calibrated based on estimates from the academic literature. Given the inherent difficulty in measuring asset class illiquidity, I rely on crude approximations for the average expected time to redeem the investment in each asset class. The timing of exit or redemption for most private asset funds is uncertain, often contingent on market conditions for IPOs, mergers, and acquisitions, which is also the reason why illiquidity is stochastic in this model. Secondary markets for private equity and hedge funds remain nascent, characterized by thin trading volumes and significant pricing discounts (Kleymenova et al., 2012; Ramadorai, 2012; Nadauld et al., 2019). For this reason, they are not considered here.

For private equity, Metrick and Yasuda (2010) report a median exit time of approximately five years, but it can extend to more than 10 years. Andonov et al. (2021) observe comparable exit times for infrastructure investments, as most investors access these assets through closed-end funds structured similarly to private equity. Bitsch et al. (2010) further highlight that while the underlying assets of infrastructure funds often have long lifespans, the funds themselves exhibit exit times similar to those of private equity funds.

Based on these findings, I adopt a calibration for the illiquidity parameter η of 1/5 and 1/10 for private equity and infrastructure funds. For Real Estate funds, Fisher and Hartzell (2016) report median exit times ranging from 4.25 to 5.5 years, supporting again a calibration of $\eta = 1/5$.

Hedge funds, in contrast, have much shorter illiquidity horizons related to gates imposed by the manager or varying lock-up periods and redemption notice requirements. Although these contractual clauses are typically known once a fund manager is selected, ex-ante they vary across funds. I calibrate their illiquidity to $\eta = 1$, aligning with the findings reported in Schaub and Schmid (2013).

Table 5: Portfolio Allocation and Welfare Metrics under Liquidity Scenarios

	Private Equity			Infrastructure			Real Estate		Diversified Hedge Funds		Macro Hedge Funds	
	Liquid	Illiquid 5Y	Illiquid 10Y	Liquid	Illiquid 5Y	Illiquid 10Y	Liquid	Illiquid	Liquid	Illiquid	Liquid	Illiquid
Fixed Income	63.20	67.02	67.99	49.21	56.78	62.94	30.57	54.87	23.07	29.13	57.97	58.25
- Short Term	30.92	48.56	53.81	47.11	51.74	55.55	9.13	39.89	8.99	15.71	47.90	48.18
- Long Term	32.27	18.47	14.18	2.10	5.03	7.39	21.44	14.99	14.08	13.41	10.07	10.07
Equity	0.19	4.66	11.17	5.20	10.17	14.13	18.02	20.43	3.34	5.29	16.47	16.50
Liquid Alternatives	0.40	11.14	11.93	16.39	14.95	13.83	0.05	4.07	14.42	14.08	13.34	13.33
Private Assets	36.15	17.09	8.82	29.12	18.03	9.01	51.31	20.55	59.13	51.46	12.13	11.84
CEC	4.59	4.31	4.14	4.13	4.09	4.02	5.25	4.60	4.24	4.21	3.95	3.95
Median Realized ξ	36.15	20.34	13.41	29.12	20.44	12.13	51.31	24.60	59.13	51.46	12.13	11.84
Median Realized c	4.32	4.09	3.94	3.95	3.92	3.86	4.83	4.31	3.98	4.02	3.81	3.81
Allocation Benefit	16.65	9.51	5.11	4.78	3.87	2.20	33.46	16.78	7.70	6.98	0.27	0.27
Misallocation Risk	-	3.69	12.49	-	0.58	5.43	-	16.68	-	0.19	-	0.00

Note. This table shows model results for a long-only investor.

Table 5 first presents the model solution for the optimal strategic allocation. Embedding illiquidity into the portfolio optimization influences the investor's consumption rate, allocation decisions, and consequent welfare. In each case, for comparison reasons, I consider first the hypothetical situation in which the private asset can be traded continuously. Comparing against this, it can be seen that considering the illiquidity risk of the private assets significantly alters the composition of the liquid sub-portfolio. The most notable shift is the substantial increase in short-term fixed-income allocations. As noted earlier, the higher cash buffers mitigate the risk of significant disruptions in consumption. The reduction in the allocation to the private asset class when illiquidity is considered is particularly pronounced for private equity, where the allocation declines from 36.15% under the liquid assumption to 17.09% for a five-year expected waiting time and further to 8.82% for a ten-year waiting time. This is accompanied by a substitution effect where the allocations to public equity and liquid alternatives (e.g., REITs) are increased, rising from zero to approximately 11.17% and 11.93%, respectively, in response to the reduced role of private equity. Similar reallocation patterns are observed for Real Estate, which tends to be substituted partially by REITs, and Infrastructure, which is partially substituted by Public Equity. Hedge funds, on the other hand, are comparatively much more liquid. They show a similar trend but to a lesser extent. Among hedge fund strategies, Diversified Hedge Funds exhibit a more pronounced substitution effect due to their higher correlation with public equity, while Macro Hedge Funds maintain relatively stable allocations. The relatively high allocation to the risk-free asset (here: short-term fixed income) is driven by the relatively high interest rate in the CMAs. I do not put additional restrictions on cash.

The inclusion of a private asset class in the portfolio, even after accounting for its illiquidity, yields measurable allocation benefits. These benefits, expressed as percentage increases in certainty equivalent consumption (CEC), range from 0.2% to 16%. The highest allocation benefit is observed for Real Estate, which provides significant diversification advantages, while the lowest benefit is for Macro Hedge Funds, reflecting their lower risk-adjusted returns (as shown in Table 5).[12] Yet, the the inclusion of illiquidity risk in the optimization significantly lowers the estimated allocation benefit from the estimate which ignores illiquidity. The shift is most notable for Private Equity, where the allocation benefit drops from 16% when only variance risk is considered, down to 5% when the expected time between liquidity events is extended up to 10 years.

As a result, ignoring illiquidity exposes investors to substantial misallocation loss. Allocating according to a liquid model leads to a 3% welfare loss for private equity assuming a five-year expected waiting time, and extends up to to 12% for a ten-year waiting time. Infrastructure investments exhibit relatively low misallocation risks for the 5-year expected waiting times but face up to a 5% welfare loss if the expected waiting time is extended to 10 years. Real Estate, possibly due to its diversification benefits, incurs

[12]The baseline CEC for a portfolio excluding private assets altogether is 3.937 per $100, serving as a benchmark against which the allocation benefits are measured.

the highest misallocation risk among private assets. Even with a five-year waiting time, welfare losses due to misallocation can reach 16%. Hedge funds demonstrate significantly lower misallocation risks.

6 Conclusion

This paper underscored the role of illiquidity when private asset classes are part of the investor's strategic allocation mix, and quantifies the degree to which they improve the certainty equivalent consumption of a long-term investor. I find that the allocation gains are tempered when illiquidity risk is properly accounted for. Ignoring it, on the other hand, can lead to overallocation and significant welfare losses, particularly for highly illiquid assets such as private equity and real estate.

The dynamic portfolio choice model presented here provides a unified framework to handle illiquid private assets. Further extensions can capture the nuances of each specific private asset class. In addition, fixed costs of investment, typically a concern for smaller investors, can be included in the framework as private assets require strong expertise and due diligence process which comes at an initial cost to develop. Also, the modeling of secondary markets was avoided here. Yet, as they become more liquid fund exit alternatives, including them in the model can be explored as well. In any case, however, the dynamic portfolio choice model presented here provides an intuitive framework for the discussion of illiquidity in the asset allocation problem, and allows the use of CMAs typically part of the institutional investor's asset allocation toolbox.

References

Andonov, A. and Rauh, J. D. 2022. The return expectations of public pension funds. *The Review of Financial Studies*, 35(8):3777–3822.

Andonov, A., Eichholtz, P., and Kok, N. 2015. Intermediated investment management in private markets: Evidence from pension fund investments in real estate. *Journal of Financial Markets*, 22:73–103.

Andonov, A., Kräussl, R., and Rauh, J. 2021. Institutional investors and infrastructure investing. *The Review of Financial Studies*, 34(8):3880–3934.

Andonov, A., Bonetti, M., and Stefanescu, I. 2023. Choosing pension fund investment consultants. *Available at SSRN 4306217*.

Ang, A. 2014, *Asset Management*. Oxford University Press.

Ang, A. and Sorensen, M. 2012. Risks, returns, and optimal holdings of private equity: A survey of existing approaches. *The Quarterly Journal of Finance*, 2(03):1250011.

Ang, A., Papanikolaou, D., and Westerfield, M. M. 2014. Portfolio choice with illiquid assets. *Management Science*, 60(11):2737–2761.

Begenau, J., Liang, P., and Siriwardane, E. 2024. The rise of alternatives.

Bitsch, F., Buchner, A., and Kaserer, C. 2010. Risk, return and cash flow characteristics of infrastructure fund investments. *EIB papers*, 15(1):106–136.

Boyle, P. P. and Lin, X. 1997. Optimal portfolio selection with transaction costs. *North American Actuarial Journal*, 1(2):27–39.

Brennan, M. J., Schwartz, E. S., and Lagnado, R. 1997. Strategic asset allocation. *Journal of Economic dynamics and Control*, 21(8-9):1377–1403.

Broeders, D. W., Jansen, K. A., and Werker, B. J. 2021. Pension fund's illiquid assets allocation under liquidity and capital requirements. *Journal of pension economics & finance*, 20(1):102–124.

Brown, G. W., Gredil, O. R., and Kaplan, S. N. 2019. Do private equity funds manipulate reported returns? *Journal of Financial Economics*, 132(2):267–297.

Brown, G. W., Ghysels, E., and Gredil, O. R. 2023. Nowcasting net asset values: The case of private equity. *The Review of Financial Studies*, 36(3):945–986.

Cai, Y., Judd, K. L., and Xu, R. 2013. Numerical Solution of Dynamic Portfolio Optimization with Transaction Costs. *NBER Working Paper No. w18709*.

Couts, S. J., Gonçalves, A. S., and Loudis, J. 2023. The subjective risk and return expectations of institutional investors. *Fisher College of Business Working Paper*, 14.

Dai, M., Jin, H., and Liu, H. 2011. Illiquidity, position limits, and optimal investment for mutual funds. *Journal of Economic Theory*, 146(4):1598–1630. ISSN 0022-0531.

Darolles, S. and Roussellet, G. 2023. Managing hedge fund liquidity risks. *Available at SSRN 5043919*.

Diamond, P. A. 1982. Aggregate Demand Management in Search Equilibrium. *Journal of Political Economy*, 90(5):881–94.

Dimmock, S. G., Wang, N., and Yang, J. 2023. The endowment model and modern portfolio theory. *Management Science*, 70(3):1554–1579.

Fisher, L. M. and Hartzell, D. J. 2016. Class differences in real estate private equity fund performance. *The Journal of Real Estate Finance and Economics*, 52:327–346.

Franzoni, F., Nowak, E., and Phalippou, L. 2012. Private equity performance and liquidity risk. *Journal of Finance*, 67(6):2341–2373.

Gennotte, G. and Jung, A. 1994. Investment Strategies under Transaction Costs: The Finite Horizon Case. *Management Science*, 40(3):385–404.

Giesecke, O. and Rauh, J. 2023. Trends in state and local pension funds. *Annual Review of Financial Economics*, 15:221–238.

Giommetti, N. and Sorensen, M. 2021. Optimal allocation to private equity. *Tuck School of Business Working Paper*, (3761243).

Gourier, E., Phalippou, L., and Westerfield, M. M. 2024. Capital commitment. *The Journal of Finance*, 79(5):3407–3457.

Gredil, O., Liu, Y., and Sensoy, B. A. 2020. Diversifying private equity. *Available at SSRN 3535677*.

Ilmanen, A., Chandra, S., and McQuinn, N. 2020. Demystifying illiquid assets: Expected returns for private equity. *The Journal of Alternative Investments*, 22(3):8–22.

Jansen, K. A. and Werker, B. J. 2022. The shadow costs of illiquidity. *Journal of Financial and Quantitative Analysis*, 57(7):2693–2723.

Judd, K. L. 1998, *Numerical Methods in Economics*. MIT Press.

Kim, J. H., Lee, Y., Kim, W. C., and Fabozzi, F. J. 2021. Mean–variance optimization for asset allocation. *The Journal of Portfolio Management*, 47(5):24–40.

Kleymenova, A., Talmor, E., and Vasvari, F. P. 2012. Liquidity in the secondaries private equity market. *Working paper, London Business School.*

Korteweg, A. and Westerfield, M. M. 2022. Asset allocation with private equity. *Foundations and Trends® in Finance*, 13(2):95–204.

Longstaff, F. A. 2001. Optimal Portfolio Choice and the Valuation of Illiquid Securities. *Review of Financial Studies*, 14(2):407–31.

Luxenberg, E., Boyd, S., van Beek, M., Cao, W., and Kochenderfer, M. Strategic asset allocation with illiquid alternatives. In *Proceedings of the third ACM international conference on AI in finance*, pages 249–256, 2022.

Magill, M. J. P. and Constantinides, G. M. 1976. Portfolio selection with transactions costs. *Journal of Economic Theory*, 13(2):245–263.

Martellini, L. and Milhau, V. 2020. Does factor investing improve investor welfare? A multi-asset perspective. *Journal of Portfolio Management*, 46(6):32–53.

Merton, R. C. 1971. Optimal consumption and portfolio rules in a continuous-time model. *Journal of Economic Theory*, 3:373–413.

Metrick, A. and Yasuda, A. 2010. The economics of private equity funds. *The Review of Financial Studies*, 23(6):2303–2341.

Miklós, K. and Ádám, S. 2002. Portfolio Choice with Illiquid Assets. Rajk László Szakkollégium Working Papers 6, Rajk László College.

Nadauld, T. D., Sensoy, B. A., Vorkink, K., and Weisbach, M. S. 2019. The liquidity cost of private equity investments: Evidence from secondary market transactions. *Journal of Financial Economics*, 132(3):158–181.

Ramadorai, T. 2012. The secondary market for hedge funds and the closed hedge fund premium. *Journal of Finance*, 67(2):479–512.

Rust, J. 1996. Numerical dynamic programming in economics. *Handbook of computational economics*, 1:619–729.

Schaub, N. and Schmid, M. 2013. Hedge fund liquidity and performance: Evidence from the financial crisis. *Journal of Banking & Finance*, 37(3):671–692.

Sefiloglu, O. 2022. In pursuit of information: Information asymmetry in private equity commitments. *Available at SSRN 4239801*.

Terhaar, K., Staub, R., and Singer, B. D. 2003. Appropriate policy allocation for alternative investments. *The Journal of Portfolio Management*, 29(3):101–110.

Zabel, E. 1973. Consumer Choice, Portfolio Decisions, and Transaction Costs. *Econometrica*, 41(2):321–35.

A Discretization & Numerical Solution Methods

This section outlines the numerical approaches used to find the reduced-form value function $H(\xi)$ and the optimal controls for the portfolio choice problem with illiquidity defined in Section 3.[13]

A.1 The trading probability and the Poisson process

Figure 6: Relationship between p and η

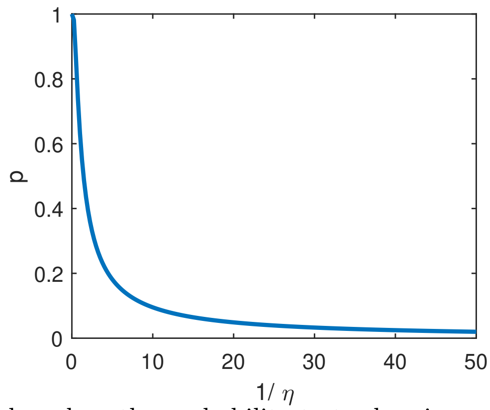

The plot shows the connection based on the probability to trade p in an illiquid asset within a year and $1/\eta$, the average waiting time in years between trades.

First, we define the probability p with which the investor trades the illiquid asset over a discrete time period Δt. This probability will be a function of the intensity η of the Poisson process that indicates the relocation opportunities. To show that formally, note that a Poisson process has stationary and independent increments, where the number of events that occur during any time increment of length Δt is Poisson distributed with mean $\eta\Delta t$. Then the probability that n events occur over the time increment can be written as: $P(N_{t+\Delta t} - N_t = n) = \mathrm{e}^{-\eta\Delta t}\frac{(\eta\Delta t)^n}{n!}$. We can then show that p, as the probability of having at least one trading event over time period Δt is such that

$$p = 1 - \mathrm{e}^{-\eta\Delta t} \tag{18}$$

[13]The model presented here and code to reproduce the results of this paper is available at https://github.com/danielkdimitrov/portfolioChoiceIlliq

Figure 6 illustrates this functional relationship over an annual horizon. It is well-known that the that $1/\eta$ represents the waiting time between two Poisson counts, so correspondingly, for a more appealing representation, I plot on the x-axis the expected time between two trades.

A.2 Discretizing the Bellamn equation:

Now, we look at time discretization of the dynamic optimization problem. The discretized Bellman equation can then be solved through value function iteration combined with standard numerical techniques.

Define the growth rate in liquid $R_{w,t+\Delta t}(c_t, \boldsymbol{\theta}_t) = \frac{W_{t+\Delta t}}{W_t}$ and illiquid wealth $R_{x,t+\Delta t} = \frac{X_{t+\Delta t}}{X_t}$ for the cases when rebalancing is not possible (i.e. $dI_t = 0$ in (5)), such that the Euler discretization of the continuous stochastic process (3) holds, ass:

$$\begin{aligned} R_{w,t+\Delta t} &= 1 + (r + \boldsymbol{\theta}_t'(\boldsymbol{\mu}_w - r\mathbb{1}) - c_t)\Delta t + \boldsymbol{\theta}_t'\boldsymbol{\sigma}_w\sqrt{\Delta t}\boldsymbol{\Delta Z}_t \\ R_{x,t+\Delta t} &= 1 + \mu_x\Delta t + \boldsymbol{\sigma}_x\sqrt{\Delta t}\boldsymbol{\Delta Z}_t \end{aligned} \tag{19}$$

where $\boldsymbol{\Delta Z}_t$ is a column vector of standard normal random variables.[14]

Then, we can define the growth in total wealth $R_{q,t+\Delta t} = \frac{Q_{t+\Delta t}}{Q_t}$, and the change in the illiquid asset share $\xi_{t+\Delta t}$ as:

$$\begin{aligned} R_{q,t+\Delta t} &= (1-\xi_t)R_{w,t+\Delta t} + \xi R_{x,t+\Delta t} \\ \xi_{t+\Delta t} &= \xi_t \frac{R_{x,t+\Delta t}}{R_{q,t+\Delta t}} \end{aligned} \tag{20}$$

Proposition: The dynamic problem defined in Section 3 can be solved through the discterized Bellman equation of the form:

$$\begin{aligned} &H(\xi_t) = \\ &\quad \max_{(\theta_t, c_t)} \left\{ u(c_t(1-\xi_t))\Delta t + \delta\left(pH^* E_{\xi_t}\left[R_{q,t+\Delta t}^{1-\gamma}\right] + (1-p)E_{\xi_t}\left[R_{q,t+\Delta t}^{1-\gamma} H(\xi_{t+\Delta t})\right]\right)\right\} \end{aligned} \tag{21}$$

[14] A Gaussian quadrature approach will be used for the space-discretization of the normal distribution and for the evaluation of the expectations in the Euler equation presented next (cf. Section A.4).

where p is the discretized probability of being able to trade next period (cf. Equation (18)), $\delta = \mathrm{e}^{-\beta \varDelta t}$ is a discount factor, $H(.)$ is the reduced value function of Equation (11), and $H^* = \max_\xi H(\xi)$.

Proof: It is easy to derive equations (20):

$$\begin{aligned} R_{q,t+\varDelta t} &= \frac{Q_{t+\varDelta t}}{Q_t} = \frac{W_t R_{w,t+\varDelta t} + X_t R_{x,t+\varDelta t}}{Q_t} \\ &= (1-\xi_t) R_{w,t+\varDelta t} + \xi R_{x,t+\varDelta t} \\ \xi_{t+\varDelta t} &= \frac{X_{t+\varDelta t}}{Q_{t+1}} = \frac{X_t}{Q_t} \frac{X_{t+\varDelta t}}{X_t} \frac{Q_t}{Q_{t+\varDelta t}} \\ &= \xi_t \frac{R_{x,t+\varDelta t}}{R_{q,t+\varDelta t}} \end{aligned}$$

The dynamic optimization problem with illiquid assets is defined through the intertemporal objective given in ((6)) and the law of motion given in (5). Using the Bellman principle of optimality we can tranform the dynamic problem into its discret time version[15]:

$$V(W_t, X_t) = \max_{(\theta_t, dI_t, c_t \in \mathcal{A})} \{u(C_t)\varDelta t + \delta E_{W_t, X_t}[V(W_{t+\varDelta t}, X_{t+\varDelta t})]\}$$

with $\delta = \mathrm{e}^{-\beta \varDelta t}$ as a discrete-time discount factor, and where the expectation is conditional on the initial liquid wealth W_t and illiquid wealth X_t at time t. Using the homothetic properties of the CRRA utility from Equation 11, we can rewrite the Bellman equatoin:

$$\begin{aligned} V(Q_t, \xi_t) &= \max_{(\theta_t, \xi_t, c_t \in \mathcal{R})} \{u(c_t(1-\xi_t)Q_t)\varDelta t + \delta E_{Q_t, \xi_t}[V(Q_{t+\varDelta t}, \xi_{t+\varDelta t})]\} \\ Q_t^{(1-\gamma)} H(\xi_t) &= \max_{(\theta_t, \xi_t, c_t \in \mathcal{R})} \{Q_t^{(1-\gamma)} u(c_t(1-\xi_t))\varDelta t + \delta E_{Q_t, \xi_t}[Q_{t+\varDelta t}^{(1-\gamma)} H(\xi_{t+\varDelta t})]\} \end{aligned}$$

[15]To get intuition on the discretization step from the classic Merton case, note that the discrete Bellman equation $V(W_t) = \sup_{(\pi_t, C_t)} \{u(C_t)\varDelta t + \mathrm{e}^{-\beta \varDelta t} E[V(W_{t+\varDelta t})]\}$ can be shown to converge to its continuous counterpart for $\varDelta t \to 0$. Multiply the equation by $\mathrm{e}^{\beta \varDelta t}$, subtract $V(W)$ from both sides and divide by $\varDelta t$ and this results in: $\frac{\mathrm{e}^{\beta \varDelta t}-1}{\varDelta t} V(W) = \sup_{(\pi_t \in \mathcal{R}^d, c_t \geq 0)} \{u(c_t) + \frac{1}{\varDelta t} E_t[V(W_{t+\varDelta t}) - V(W_t)]\}$

Let $\varDelta t \to 0$, then $\mathrm{e}^{\beta \varDelta t} \to 1$ and also by the L'Hôpital rule we have that $\frac{\mathrm{e}^{\beta \varDelta t}-1}{\varDelta t} \to \beta$. As a result $\frac{1}{\varDelta t} E_t[V(W_{t+\varDelta t}) - V(W_t)] \to E_t[dV]$ which makes discretized equation equivalent to the continuous time version: $\sup_{(\boldsymbol{\pi}_t, C_t)} \mathrm{e}^{-\beta t} u(C_t) + E\left[d(\mathrm{e}^{-\beta t} V(W_t))\right] dt = 0$

The investor will set $\xi_{t+\Delta t} = \xi^*$ whenever trading is possible, coming to the top of the value function, $H(\xi)$. If trading is not possible, the investor cannot rebalance and is stuck with suboptimal levels of illiquid holdings $\xi_{t+\Delta t}$, and the ratio will float away in a random direction from last period's value as the prices of the two risky assets move. Since that case is suboptimal, the value function will be lower and at $H(\xi_{t+\Delta t})$. This is illustrated in Figure 7.

Figure 7: Dynamic Asset Allocation and State Transition

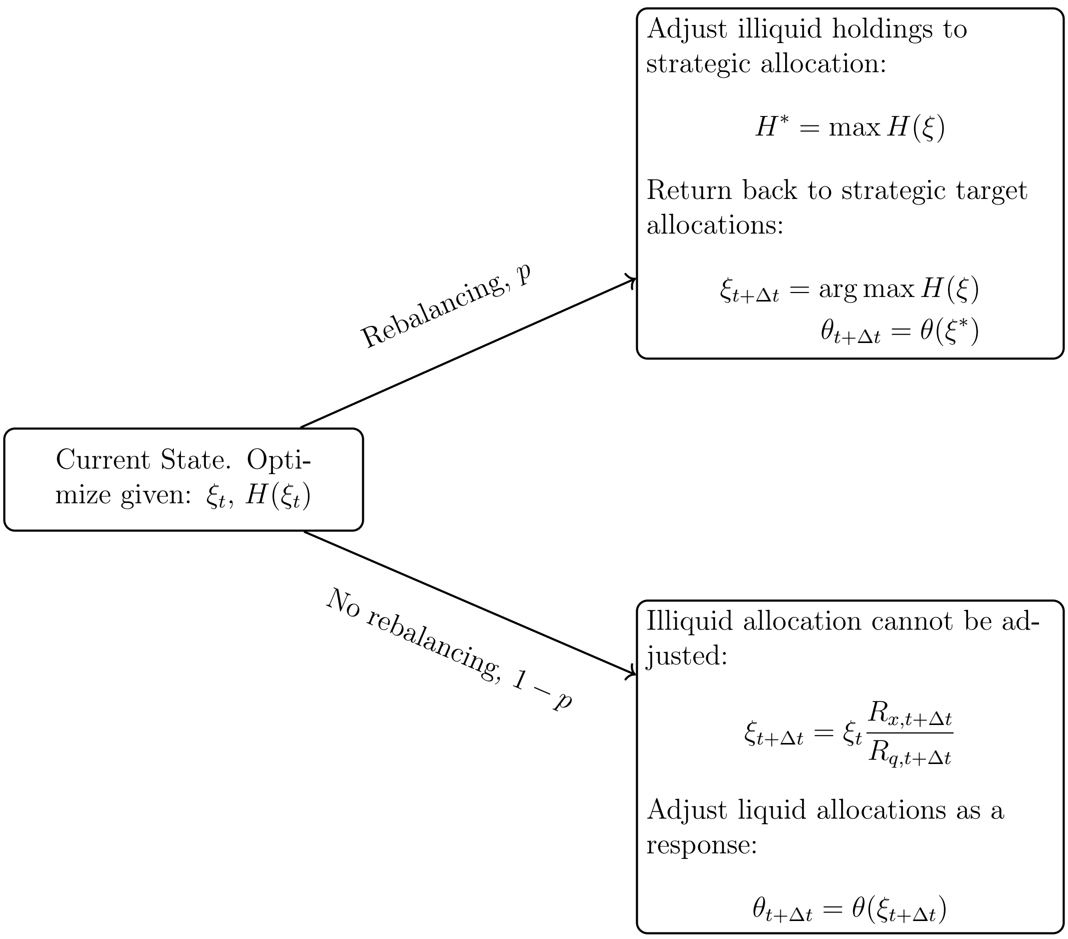

This chart illustrates the dynamics behind the optimal choice problem. In the coming period, the illiquid asset share floats freely to $\xi_{t+\Delta t}$. With probability p, the investor can trade in the illiquid asset and set it back to the optimal target of ξ^* by maximizing the known function $H(\xi)$. With probability $1-p$, the investor cannot trade and is stuck with the illiquid asset share of $\xi_{t+\Delta t}$.

Combining the two, we can write the Bellman equation as:

$$Q_t^{(1-\gamma)} H(\xi_t) =$$
$$\max_{(\theta_t, dI_t, c_t \in \mathcal{R})} \left\{ Q_t^{(1-\gamma)} u(c_t(1-\xi_t))\Delta t + \delta\Big(pE_{Q_t}[Q_{t+\Delta t}^{(1-\gamma)}]H^* + (1-p)E_{Q_t}[Q_{t+\Delta t}^{(1-\gamma)} H(\xi_{t+\Delta t})]\Big) \right\}$$

Note, that by canceling out Q_t and by embedding it in the expectations the conditional part of the expectation with respect to Q can be dropped and we arrive to Equation (21). □

A.3 Value Function Iteration:

Based on the discretization from Annex A.2, we can solve the portfolio choice dynamic problem through value function iteration. Discretizing ξ and evaluating the system one period ahead will allow us to iterate (21) until the iterative approximation of the value function $H(\xi)$ converges. The procedure will eventually yield a numerical approximation of the value function and the optimal solution for the policy functions $c(\xi)$ and $\theta(\xi)$. So, the goal is to find the approximating function $\tilde{H}(.)$ evaluated on a fixed grid $\tilde{\xi}$ which best approximates the true theoretical function $H(\xi)$ underlying the HJB equation (C.2). We use the following iterative procedure:

Initialization: Discretize the random space (the random variables ΔZ_1 and ΔZ_2 in (19)) through a simulation or strategically selected (Gaussian) quadrature points (see Annex A.4).

Select an approximation grid of N gridpoints for ξ_t: $\tilde{\xi} = \{\xi_1, ..., \xi_N\} \in [0;1)$, $j = 1, .., N$. I use $N = 20$. Select a class of approximating functions $\tilde{H}(\boldsymbol{a}; \tilde{\xi})$ which will approximate the true value function $H(\xi)$ and initialize the functional parameters $\boldsymbol{a}$. In particular I use a cubic spline due to its flexibility to capture strong curvature of the $H()$ function at the upper edge of ξ_t. Fitting the spline over the logarithmized values of the evaluated function also improves the convergences.

Select an initial guess for the maximum $\tilde{H}^*$ of the value function. As a starting point for the iteration we use the analytical two-asset Merton solution. We can then initiate the following iterative algorithm.

1. **Optimization:** For each ξ_j in the grid evaluate numerically optimal consumption and liquid asset allocation:

$$c^{*,k}, \theta^{*,k+1} = \arg\min \Big\{ u(c(1-\xi_j))\Delta t + \delta \Big(p\tilde{H}^* E \left[\hat{q}(c,\theta,\xi_j)^{1-\gamma} \right] \\ + (1-p) E \left[\tilde{H}\left(\boldsymbol{a}^k; \hat{\xi}(c,\theta,\xi_j) \right) \hat{q}(c,\theta,\xi_j)^{1-\gamma} \right] \Big) \Big\}$$

   where $\hat{\xi}()$ and $\hat{q}()$ are next-period's dynamics calculated through (20), and $k = 1,...,p$ is a counter measuring the iteration run.

2. **Update:** For each ξ_j and the optimal control policies found in the previous step update values of the value function that lie on the grid. Update the fit of the approximation function $\tilde{H}(\boldsymbol{a}^{k+1};\xi)$ based on the new values. Update $\tilde{H}^{*,k+1} = \arg\max_\xi \tilde{H}(\boldsymbol{a}^{k+1};\xi)$.

3. **Stopping:** The algorithms stops if $\left\| \ln(-\tilde{H}(\boldsymbol{a}^{k+1};\xi)) - \ln(-\tilde{H}(\boldsymbol{a}^{k};\xi)) \right\|^2 < \epsilon$, otherwise we go to **Step 1**. I use $\epsilon = 0.1^6$

A.4 Gauss-Hermite Quadrature

I use quadrature approximation to evaluate the expectation terms in the numerical section of this paper. Multi-dimensional quadrature methods are less common, so I provide here a discussion of this approach, based on (Rust, 1996; Judd, 1998; Cai et al., 2013) and show how the recipe can be adapted to the discretized Bellman equation defined in (21).

Univariate case: We can start with a discussion of a one-dimensional quadrature. This will be used to generalize the problem to multiple dimensions. Gaussian quadrature approximates an integral of the form:

$$\int_a^b f(x)w(x)\,dx \approx \sum_{i=1}^m w_i f(x_i)$$

where $w(x)$ is a weight function, x_i are the quadrature nodes, w_i are the quadrature weights, and m is the number of quadrature points.

When dealing with integrals involving a normally distributed random variable (or the logarithm of a log-normally distributed variable), Gauss-Hermite (GH) quadrature is particularly useful. It applies a weight function $w(x) = e^{-x^2}$ and integrates over the entire real line. The nodes x_i are the roots of the Hermite polynomial, and the weights w_i are determined accordingly to accurately approximate the integral.

Note, however, that when evaluating the expectation of $f(y)$ for a random variable y which is normally distributed with $y \sim N(\mu, \sigma)$ we have

$$\mathbb{E}(f(y)) = (2\pi\sigma^2)^{-1/2} \int_{-\infty}^{\infty} f(y) e^{-\frac{(y-\mu)^2}{2\sigma^2}} dy$$

To reconcile this with the GH approximation, we first use a change of variable $y = \sqrt{2}\sigma x + \mu$ and then apply the given quadrature approximation such that

$$\mathbb{E}(f(\sqrt{2}\sigma x + \mu)) = (\pi)^{-1/2} \int_{-\infty}^{\infty} f(\sqrt{2}\sigma x + \mu) e^{-x^2} dx \approx \frac{1}{\sqrt{\pi}} \sum_{i=1}^{m} w_i f(\sqrt{2}\sigma x_i + \mu)$$

Multivariate case: Similarly, for a multivariate normal vector $\boldsymbol{y} \sim N(\boldsymbol{\mu}, \boldsymbol{\Sigma})$, where $\boldsymbol{\mu}$ is an $n \times 1$ mean vector and $\boldsymbol{\Sigma}$ is a positive semi-definite covariance matrix, and $f(\boldsymbol{x}) : \mathbb{R}^n \to \mathbb{R}$ a scalar-valued function, the expectation $\mathbb{E}[f(\boldsymbol{y})]$ can be evaluated using a change of variable after performing a Cholesky decomposition $\boldsymbol{\Sigma} = \boldsymbol{\sigma}\boldsymbol{\sigma}^\top$. By substituting $\boldsymbol{y} = \sqrt{2}\boldsymbol{\sigma}\boldsymbol{x} + \boldsymbol{\mu}$, the integral

$$\mathbb{E}[f(\boldsymbol{Y})] = \frac{1}{(2\pi)^{N/2} |\boldsymbol{\Sigma}|^{1/2}} \int_{\mathbb{R}^N} f(\boldsymbol{y}) e^{-\frac{1}{2}(\boldsymbol{y}-\boldsymbol{\mu})^\top \boldsymbol{\Sigma}^{-1} (\boldsymbol{y}-\boldsymbol{\mu})} d\boldsymbol{y}$$

can be transformed to:

$$\mathbb{E}[f(\boldsymbol{Y})] = \frac{1}{\pi^{N/2}} \int_{\mathbb{R}^n} f(\sqrt{2}\boldsymbol{\sigma}\boldsymbol{x}_i + \boldsymbol{\mu}) e^{-\boldsymbol{x}^\top \boldsymbol{x}} d\boldsymbol{x}$$

where $\boldsymbol{x}_i$ is a $n \times 1$ vector quadrature node for $i = 1, \ldots, m$.

Then, in the multi-dimensional space, we can use the quadrature product rule to perform the approximation

$$\mathbb{E}[f(\boldsymbol{Y})] \approx \frac{1}{\pi^{n/2}} \sum_{i_1=1}^{m} \cdots \sum_{i_n=1}^{m} w_{i_1} \dots w_{i_n} \cdot f\left(\sqrt{2}\boldsymbol{\sigma}\boldsymbol{x}_{i_1,i_2,\dots,i_n} + \boldsymbol{\mu}\right) = \tag{22}$$

where $\boldsymbol{x}_{i_1,i_2,\dots,i_n} = \begin{pmatrix} x_{i_1}, & x_{i_2}, & \dots, & x_{i,n} \end{pmatrix}'$ is a vector representing the i-th multivariate quadrature node.[16] In particular, for further clarity we can write

$$f\left(\sqrt{2}\boldsymbol{\sigma}\boldsymbol{x}_{i_1,i_2,\dots,i_n} + \boldsymbol{\mu}\right) \equiv f\begin{pmatrix} \sqrt{2}\left(\sigma_{11}x_{i_1}\right) + \mu_1, \\ \sqrt{2}\left(\sigma_{21}x_{i_1} + \sigma_{22}x_{i_2}\right) + \mu_2, \\ \cdots \\ \sqrt{2}\left(\sigma_{11}x_{i_1} + \dots + \sigma_{nn}x_{i_n}\right) + \mu_n \end{pmatrix}$$

with μ_i as elements of the vector of expectations, and σ_{11},$\sigma_{22}, \dots$ as elements of the $\boldsymbol{\sigma}$ matrix.

With this in mind, it becomes trivial to evaluate the expectation terms in (21) using the following steps:

1. Draw m weights and nodes from a uni-variate GH quadrature as w_{i_j} and x_{i_j} where $i = 1, \dots, m$ is the index of the quadrature points. The index j of the respective risk factor[17] will come into play in the next step.

2. Construct in a $m \times n$ matrix the Cartesian product of n copies of the univariate GH nodes form step (1). Each row of this matrix represents the transposed $\boldsymbol{x}_i$ quadrature node vector defined earlier. Denote by $\boldsymbol{z}_{1_j,2_j,\dots,m_j} = \begin{pmatrix} x_{1_j}, & x_{2_j}, & \dots, & x_{m,j} \end{pmatrix}'$ the j-th column from that matrix.

3. Similarly, construct the Cartesian product of n copies of the univariate GH weights form step (1). This produces the weights w_{j_k} needed in Equation (22).

[16]Here we assume that the same number m of nodes is used to evaluate each risk factor. In general, this need not be the case, and different number of nodes could be drawn for each risk factor.

[17]Which in our case corresponds to dZ_j, or the j-th element of the multivariate Brownian motion vector $\boldsymbol{dZ}$.

4. In the discretized dynamic Equation (19) set $\Delta Z_{j,t} \equiv \sqrt{2}\boldsymbol{z}_{1_j,2_j,\ldots,m_j}$ for each $\Delta Z_{j,t}$ being an element of the vector of discretized Brownian motions $\boldsymbol{\Delta Z_t}$ and evaluate the gross return of the liuqid and corresponding the illiquid wealth. This produces an $m \times 1$ vector of returns for each wealth process, evaluated at the corresponding multivariate quadrature nodes.

5. Evaluate $R_{q,t+\Delta t}, \xi_{t+\Delta t}$ and $H(\xi_{t+\Delta t})$ at each node j.

6. Finally, evaluate the expectations terms in Equation 21 through the quadrature approximation defined in (22).

B Benchmark Liquid Market: The Merton Model

B.1 Optimization

First, consider the benchmark case where all assets can be continuously traded. A representative investor holds a liquid financial portfolio out of which she can withdraw (consume) continuously the rate c_t. The investor has control over the asset allocation by setting the risky asset investment proportions collected in the column vector $\boldsymbol{\pi}_t$.[18] The wealth dynamics are then determined by the return of the portfolio net of the consumption rate:

$$\frac{dW_t}{W_t} = (r + \boldsymbol{\pi}_t'(\boldsymbol{\mu} - r\mathbb{1}) - c_t)dt + \boldsymbol{\pi}_t'\boldsymbol{\sigma}\boldsymbol{dZ}_t \tag{23}$$

Subject to these wealth dynamics, the investor optimizes over time her expected lifetime utility:

$$V(W_t) = \sup_{(\pi_s, C_s)} E_t \int_t^\infty \mathrm{e}^{-\beta(s-t)} u(C_s) ds \tag{24}$$

giving rise to the indirect utility of wealth function $V(W_t)$, with β a subjective discount rate, and $t \leq s$.

Applying the Bellman principle, we can derive the Hamilton-Jacobi-Bellman (HJB)

[18] More generally, $\boldsymbol{\pi}_t$ can be interpreted as exposures to factor excess returns.

equation:

$$
\begin{aligned}
&\mathcal{L}^C + \mathcal{L}^\pi - \beta V = 0 \\
&\quad \mathcal{L}^C = \sup_{C_t} \Big\{ u(C_t) - C_t V_W \Big\} \\
&\quad \mathcal{L}^\pi = \sup_{\boldsymbol{\pi}_t} \Big\{ \left(r + \boldsymbol{\pi}_t'(\mu - r\mathbb{1})\right) V_W W_t + \frac{1}{2} V_{WW} W_t^2 \boldsymbol{\pi}_t' \boldsymbol{\Sigma} \boldsymbol{\pi}_t \Big\}
\end{aligned} \tag{25}
$$

where V_W and V_{WW} are the first- and second-order partial derivatives of the value function with respect to wealth.

Through a guess and verify strategy (cf. Annex B.3), the value function can then be determined in closed form as

$$V(W_t) = \left(\frac{1}{c}\right)^\gamma \frac{W_t^{1-\gamma}}{1-\gamma} \tag{26}$$

where $c = C_t/W_t$ is the optimal consumption rate which can be shown to be fixed over time and given by

$$c = \frac{\beta + r(\gamma - 1)}{\gamma} + \frac{1}{2}\frac{\gamma - 1}{\gamma^2} \|\boldsymbol{\lambda}\|^2 \tag{27}$$

In this setting, the investor can trade continuously and thus can always keep allocations at these base levels. Optimizing over $\boldsymbol{\pi}$ provides the optimal asset allocation vector:

$$\boldsymbol{\pi} = -\frac{V_W}{W_t V_{WW}} \boldsymbol{\Sigma}^{-1}(\boldsymbol{\mu} - \boldsymbol{r}\mathbb{1}) = \frac{1}{\gamma}(\boldsymbol{\sigma}')^{-1}\boldsymbol{\lambda} \tag{28}$$

The fraction $-\frac{V_W}{W V_{WW}} = \frac{1}{\gamma}$ defines the investor's relative risk tolerance given an indirect utility $V(W)$. The optimal risky allocation then is determined through the interaction of the investor's risk tolerance with the price of risk of each specific asset in the investment universe.

B.2 The HJB equation and optimal solution

In order to derive the continuous-time Bellman equation, we examine the value function defined in (24) over a short time period Δt. Assuming that the strategies for $\boldsymbol{\pi}_s$ and C_s are set in advance and stay constant for the time interval $s \in [t, t+\Delta t)$, and applying the Bellman principle of optimality, we can split today's value function into an optimizing decision over the upcoming time span (from t until $t + \Delta t$) and an optimal strategy afterwards:

$$V(W_t) = \sup_{(\boldsymbol{\pi}_s, C_s)} \left\{ \int_t^{t+\Delta t} \mathrm{e}^{-\beta(s-t)} u(C_s) ds \right\} + \mathrm{e}^{-\beta \Delta t} E[V(t+\Delta t, W_{t+\Delta t})] \tag{29}$$

Note that the time subscript from the expectation has been dropped, as the wealth dynamics are driven by independent random shocks, implying that knowledge of the present does not help in forecasting the expected value function, so the unconditional expectation can be used instead of the conditional.

Multiplying both sides by $\frac{1}{\Delta t}\mathrm{e}^{\beta \Delta t}$ and rearranging:

$$\frac{\mathrm{e}^{\beta \Delta t} - 1}{\Delta t} V(W_t) = \sup_{(\boldsymbol{\pi}_s, C_s)} \frac{1}{\Delta t} \left\{ \int_t^{t+\Delta t} \mathrm{e}^{-\beta(s-t-\Delta t)} u(C_s) ds \right\} + \frac{1}{\Delta t} E\Big[V(W_{t+\Delta t}) - V(W_t)\Big]$$

We can evaluate the above equation for $\Delta t \to 0$. First, the by L'Hopital rule we have that $\lim_{\Delta \to 0} \frac{e^{\beta \Delta t - 1}}{\Delta t} = \beta$. Second, $\lim_{\Delta \to 0} \frac{1}{\Delta t} \int_t^{t+\Delta t} f(s) ds = f(t)$. Using the definition of a drift term in a stochastic differential equation by denoting it as $E[dV(t, W_t]$ we get the continuous time Bellman equation as

$$\beta V(t, W_t) = \sup_{(\boldsymbol{\pi}_t, C_t)} \{u(C_t)\} + E\Big[dV(t, W_t)\Big] \tag{30}$$

Apply the Itô rule on the stochastic term $dV(t, W_t)$ in (30) and substitute in the budget constraint for dW_t

$$dV = V_W dW_t + 1/2 V_{WW} [dW_t]^2$$

$$= -C_t V_W dt + V_W W_t (rdt + \boldsymbol{\pi}_t'(\boldsymbol{\mu} - r\mathbb{1})dt + \boldsymbol{\pi}_t'\boldsymbol{\sigma}\boldsymbol{dZ}_t) + \frac{1}{2}V_{WW}W^2\boldsymbol{\pi}_t'\boldsymbol{\Sigma}\boldsymbol{\pi}_t dt$$

Using the fact that $E[\boldsymbol{dZ}] = \mathbf{0}$ we can derive the drift term of the Bellman equation as

$$E\left[dV(t, W_t)\right] dt = \left[-C_t V_W + V_W W_t (r + \boldsymbol{\pi}_t'(\boldsymbol{\mu} - r\mathbb{1})) + \frac{1}{2}V_{ww}W^2\boldsymbol{\pi}_t'\boldsymbol{\Sigma}\boldsymbol{\pi}_t\right] dt$$

which after substitution yields the HJB equation of Proposition (33):

$$\beta V(t, W_t) = \sup_{(\boldsymbol{\pi}_t, C_t)} u(C_t) - C_t V_W + V_W W_t (r + \boldsymbol{\pi}_t'(\boldsymbol{\mu} - r\mathbb{1})) + \frac{1}{2}V_{ww}W^2\boldsymbol{\pi}_t'\boldsymbol{\Sigma}\boldsymbol{\pi}_t$$

B.3 Solving for the value function

We are using the verification approach for solving the HJB equation. This involves first solving the optimization part and finding the optimal $\boldsymbol{\pi}$ and C with the yet unknown value function.As a second step, we solve the resulting HJB equation by making a guess for the value function.

We can derive optimal consumption as:

$$\begin{aligned} u'(C_t) &= V_W \\ \implies C_t &= (V_W)^{-\frac{1}{\gamma}} \end{aligned} \tag{31}$$

This is the Envelope Theorem, implying that at optimality the marginal utility from consuming a little more needs to be the same as the marginal value of investing a little more.

Similarly, the optimal allocation is

$$\boldsymbol{\pi} = -\frac{V_W}{W_t V_{WW}}(\boldsymbol{\sigma}')^{-1}\boldsymbol{\lambda} \tag{32}$$

Substituting the optimal consumption and allocation terms, (31) and (32), in (25) simplifies the HJB equation to:

$$\beta V = \frac{\gamma}{1-\gamma} V_W^{1-1/\gamma} + rW_t V_W - \frac{1}{2}\frac{V_W^2}{V_{WW}} \|\boldsymbol{\lambda}\|^2 \tag{33}$$

where $\|.\|^2$ represents the norm of a vector.

This second order Partial Differential Equation can be solved by making a guess for the value function of the form

$$V(W_t, t) = g(t)^\gamma \frac{W_t^{1-\gamma}}{1-\gamma}$$

Substituting in (33) verifies that the guess solves the PDE for $g(t) = \frac{1}{A}$, where

$$\begin{aligned} A &\equiv \frac{\beta + r(\gamma-1)}{\gamma} + \frac{1}{2}\frac{\gamma-1}{\gamma^2}\|\boldsymbol{\lambda}\|^2 \\ &= \frac{\beta + r(\gamma-1)}{\gamma} + \frac{1}{2}\frac{\gamma-1}{\gamma^2}(\boldsymbol{\mu} - r\mathbf{1})'(\boldsymbol{\sigma}\boldsymbol{\sigma}')^{-1}(\boldsymbol{\mu} - r\mathbf{1}) \end{aligned} \tag{34}$$

The optimal consumption share is thus

$$c = \frac{C_t}{W_t} = \frac{u'(V_W)^{-1}}{W_t} = A$$

where we make use of the Envelope Theorem in Equation (31), and $u'(.)^{-1}$ indicates the inverse function of the first derivative of $u(.)$. Note that $g(t)$ is a constant function. In the finite horizon case, it will be a deterministic function of time.

C Dynamic Model with Illiquidity: Proofs and Derivations

C.1 Illiquid market: Homogeneity of the value function

The proof follows from Ang et al. (2014). For CRRA utility in particular, the value function $V(W_t, X_t)$ is homogeneous of degree $1-\gamma$, such that $V(kW_t, kX_t) = k^{1-\gamma} V(W_t, X_t)$

for any $k > 0$. This is a direct consequence of the fact that the budget constraint dynamics are linear in wealth and have constant moments, independent of the corresponding wealth states. Then it is reasonable to accept that for an optimal solution $\{W_s^*, X_s^*, dI_s^*, c_s^*, \theta_s^*\}$ also $\{kW_s^*, kX_s^*, kdI_s^*, c_s^*, \theta_s^*\}$ will be optimal as well for any $k > 0$, so that scaling both liquid and illiquid wealth up or down by the same number does not change the optimal investment and consumption rates given that we also scale the wealth transfers dI by the same number. As a result, we can write

$$V(kW_t, kX_t) = \sup_{\theta, dI, c} E_t \left[\int_t^\infty \mathrm{e}^{-\beta(s-t)} \frac{(kc_s(1-\xi_s)W_s)^{1-\gamma}}{1-\gamma} ds \right] = k^{1-\gamma} V(W_t, X_t)$$

$$\iff V(W_t, X_t) = \left(\frac{1}{k}\right)^{1-\gamma} V(kW_t, kX_t)$$

Then, setting $k = 1/(W_t + X_t)$ we get

$$V(W_t, X_t) = (X_t + W_t)^{1-\gamma} V((1-\xi), \xi) = (X_t + W_t)^{1-\gamma} H(\xi)$$

where ξ is the portion of total wealth invested in the illiquid asset x and $(1-\xi)$ is the portion invested in the liquid asset. The additional proof that $H(\xi)$ is concave is available in (Ang et al., 2014).

C.2 Deriving the HJB equation

Here we derive the HJB equation for the illiquid-asset problem, starting with the continuous time Bellman equation established in (30):

$$\beta V(X_t, W_t) = \sup_{(\xi_t, \theta_t, C_t)} \{u(C_t) + E[dV(X_t, W_t)]\}$$

Making use of the Ito rule for jump processes, we can write the drift of the equation as:

$$E[dV] = E\left[V_w dW^c + V_X dX^c + \frac{1}{2}\left(V_{WW}[dW^c]^2 + V_{XX}[dX^c]^2 + 2V_{WX}[dX^c dW^c]\right) + (V^* - V)dN\right]$$

where we denote as dX^c and dW^c the continuous portion of the wealth dynamics. Using the Ito rule, then we get the corresponding quadratic variation terms:

$$
\begin{aligned}
[dW_t^c]^2 &= W_t^2 \boldsymbol{\theta}_t' \boldsymbol{\sigma}_w \boldsymbol{\sigma}_w' \boldsymbol{\theta}_t dt \\
[dX_t^c]^2 &= X_t^2 \boldsymbol{\sigma}_x \boldsymbol{\sigma}_x' dt \\
[dW_t^c dX_t^c] &= W_t X_t \boldsymbol{\theta}_t' \boldsymbol{\sigma}_w \boldsymbol{\sigma}_x' dt
\end{aligned}
$$

since we know that

$$
\begin{aligned}
dW_t^c &= W_t^c \left((r + \boldsymbol{\theta}_t'(\boldsymbol{\mu}_w - r\mathbb{1}) - c_t)dt + \boldsymbol{\theta}_t' \boldsymbol{\sigma}_w \boldsymbol{dZ} \right) \\
dX_t^c &= X_t^c \left(\mu_x dt + \boldsymbol{\sigma}_x \boldsymbol{dZ}_t \right)
\end{aligned}
$$

and denoting the jump size in the value function when a liquidity opportunity arises as $V^* - V(W_t, X_t)$, such that the expected jump size over a short period of time is $\eta(V^* - V(W_t, X_t))dt$. Note that whenever the Poisson jump process hits, we have inferred that the value function jumps to $V^* = (W_t + X_t)^{1-\gamma} H^*$.

This yields the given HJB equation

$$
\mathcal{L}^C + \mathcal{L}^\theta + \mathcal{L} - \beta V(W_t, X_t) = 0
$$

where

$$
\begin{aligned}
\mathcal{L}^C &= \sup_{C_t} \left\{ u(C_t) - C_t V_W \right\} \\
\mathcal{L}^\theta &= \sup_{\theta_t} \left\{ (r + \boldsymbol{\theta}_t'(\boldsymbol{\mu}_w - r\mathbb{1}) V_W W_t + \frac{1}{2} V_{WW} W_t^2 \boldsymbol{\theta}_t' \boldsymbol{\sigma}_w \boldsymbol{\sigma}_w' \boldsymbol{\theta}_t + V_{WX} W_t X_t \boldsymbol{\theta}_t' \boldsymbol{\sigma}_w \boldsymbol{\sigma}_x' \right\} \\
\mathcal{L} &= V_X \mu_x + \frac{1}{2} V_{XX} X^2 \boldsymbol{\sigma}_x \boldsymbol{\sigma}_x' + \eta \left(V^* - V(W_t, X_t) \right)
\end{aligned}
$$

To solve for consumption and liquid investment in terms the illiquid asset holdings, we apply the substitutions

$$\xi_t = \frac{X_t}{W_t + X_t}$$
$$V(W_t, X_t) = (W_t + X_t)^{1-\gamma} H(\xi_t)$$

such that

$$\begin{aligned}
V_W &= (W+X)^{-\gamma}\left((1-\gamma)H(\xi) - \xi H'(\xi)\right)\\
V_X &= (W+X)^{-\gamma}\left((1-\gamma)H(\xi) + (1-\xi)H'(\xi)\right)\\
V_{WW} &= (W+X)^{-\gamma-1}\left(-\gamma(1-\gamma)H(\xi) + 2\xi\gamma H'(\xi) + \xi^2 H''(\xi)\right)\\
V_{XX} &= (W+X)^{-\gamma-1}\left(-\gamma(1-\gamma)H(\xi) - 2(1-\xi)\gamma H'(\xi) + (1-\xi)^2 H''(\xi)\right)\\
V_{WX} &= (W+X)^{-\gamma-1}\left(-\gamma(1-\gamma)H(\xi) - 2(1-\xi)\gamma H'(\xi) - (1-\xi)H''(\xi)\xi\right)
\end{aligned}$$

The partial derivatives are implied using the Chain Rule such that $\frac{\partial\xi}{\partial X} = \frac{1-\xi}{W+X}$ and $\frac{\partial\xi}{\partial W} = -\frac{\xi}{W+X}$, where $H'(\xi_t)$ and $H''(\xi_t)$ denote the first and second partial derivatives of $H(\xi)$ with respect to ξ. Substituting these in the HJB equation we can solve for optimal consumption

$$c_t^* = \Big((1-\gamma)H(\xi_t) - H'(\xi_t)\xi_t\Big)^{-\frac{1}{\gamma}}(1-\xi_t)^{-1}$$

and optimal liquid risk asset investment

$$\theta_t^* = -\frac{k_1 H(\xi_t) + k_2 H'(\xi_t) + k_3 H''(\xi_t)}{k_4 H(\xi_t) + k_5 H'(\xi_t) + k_6 H''(\xi_t)}$$

where $k_1, .., k_6$ are known constants defined by the market parameters and the investor's risk aversion such that

$$\begin{aligned}
k_1 &= -(1-\gamma)(\mu_1 - r) + \gamma(1-\gamma)\sigma_2\rho\sigma_1\xi\\
k_2 &= (\mu_1 - r)\xi - \sigma_2\sigma_1\rho\xi\gamma(2\xi - 1)
\end{aligned}$$

$$k_3 = -\sigma_2\sigma_1\rho\xi^2(1-\xi)$$

$$k_4 = -\gamma(1-\gamma)(1-\xi)\sigma_1^2$$

$$k_5 = 2\gamma\xi(1-\xi)\sigma_1^2$$

$$k_6 = \xi^2(1-\xi)\sigma_1^2$$

Note that this also implies that investment and hedging curvature terms ($\Phi(\xi)$ and respectively $\Psi(\xi)$ in (13)) can be written as a function of ξ_t such that:

$$\Phi(\xi) = \left(-\frac{V_W}{V_{WW}W_t}\right) = \frac{1}{1-\xi}\left(\frac{(1-\gamma)H(\xi) - \xi H'(\xi)}{-\gamma(1-\gamma)H(\xi) - 2(1-\xi)\gamma H'(\xi) + (1-\xi)^2 H''(\xi)}\right)$$
$$\Psi(\xi_t) = -\frac{V_{WX}X_t}{V_{WW}W_t} = \frac{-\gamma(1-\gamma)H(\xi) - 2(1-\xi)\gamma H'(\xi) - (1-\xi)H''(\xi)\xi}{-\gamma(1-\gamma)H(\xi) - 2(1-\xi)\gamma H'(\xi) + (1-\xi)^2 H''(\xi)}$$

DeNederlandscheBank
EUROSYSTEEM

De Nederlandsche Bank N.V.
Postbus 98, 1000 AB Amsterdam
020 524 91 11
dnb.nl